

# TECHNICAL NOTE

## D-1069

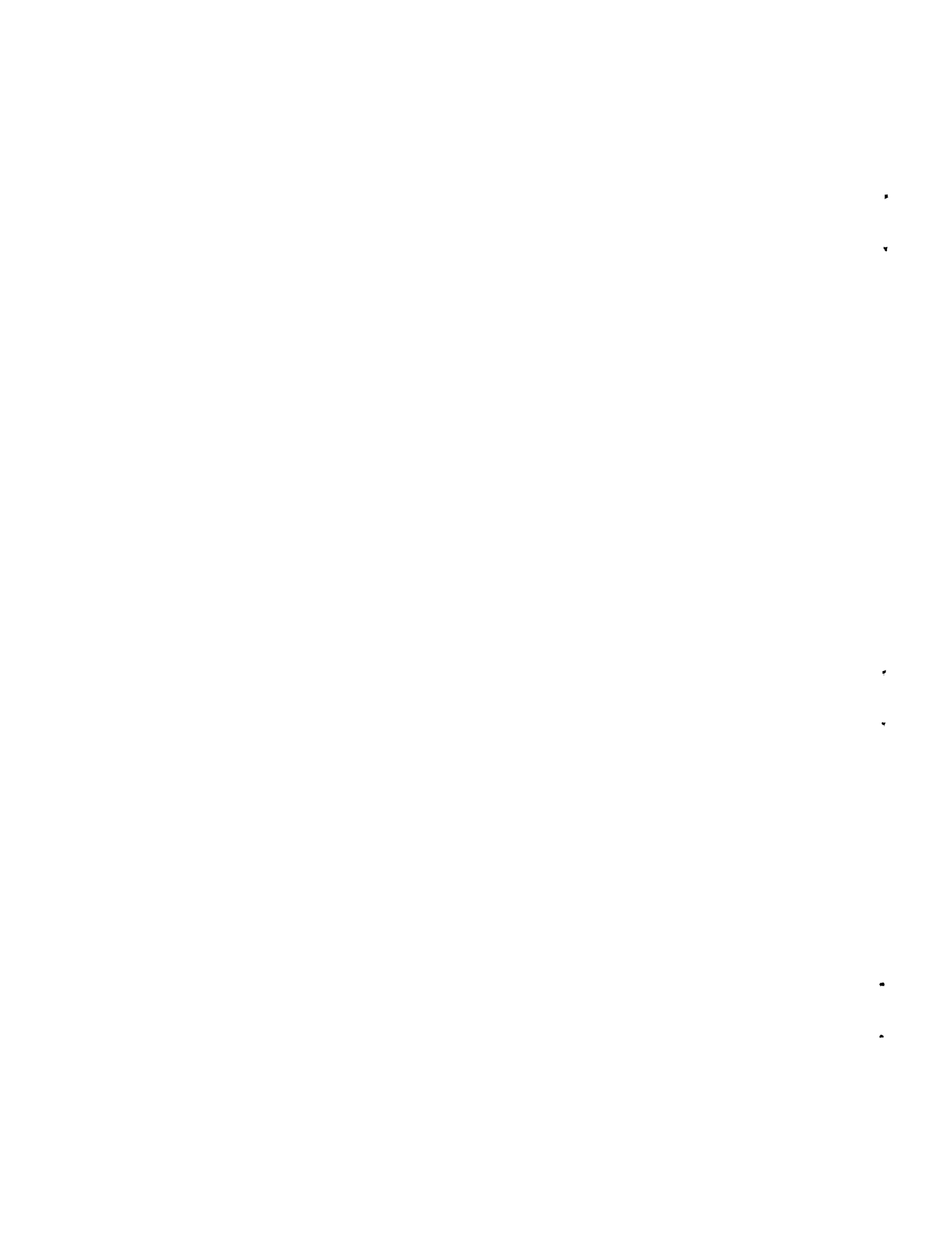
EFFECTS OF FLIGHT CONDITIONS AT BOOSTER  
SEPARATION ON PAYLOAD WEIGHT IN ORBIT

By Richard D. Nelson

Ames Research Center  
Moffett Field, Calif.

NATIONAL AERONAUTICS AND SPACE ADMINISTRATION  
WASHINGTON

November 1961



## NATIONAL AERONAUTICS AND SPACE ADMINISTRATION

## TECHNICAL NOTE D-1069

EFFECTS OF FLIGHT CONDITIONS AT BOOSTER  
SEPARATION ON PAYLOAD WEIGHT IN ORBIT

By Richard D. Nelson

## SUMMARY

A study of the principal flight parameters at booster<sup>1</sup> separation was conducted to find the effect of each on the weight of the payload boosted into an earth orbit along a zero drag gravity turn trajectory. The parameters considered include Mach number (3 to 9), flight-path angle ( $10^{\circ}$  to  $55^{\circ}$ ), altitude (90,000 and 350,000 ft), inert weight ratio (0.05 to 0.15), and thrust-weight ratio (1.5 to 2.5), with a specific impulse of 289 seconds. Both transfer ellipse and direct orbit trajectories were considered.

With either trajectory method, payload weight was highest for low initial flight-path angles and high initial Mach numbers. Of course, high initial Mach numbers require greater energy expenditures from the booster. Changes in initial altitude had little effect on payload weight, and only small gains were evident when thrust-weight ratio was increased.

## INTRODUCTION

Several studies have been made of the recovery of booster vehicles (e.g., refs. 1 and 2). The performance required of a recoverable booster vehicle depends on the flight conditions at booster separation. The purpose of this study is to determine the payload weight for various combinations of the principal flight parameters at booster separation for a range of orbital altitudes. These flight parameters apply for launches from air-breathing boosters as well as separation from rocket boosters.

Trajectories have been computed to show the effects of altitude, velocity, flight-path angle, and thrust after booster detachment on the payload weight in an earth orbit. The results presented consider only one vehicle but have been broadened in application by the introduction of an inert weight ratio concept. No attempt has been made to optimize either the vehicle or the trajectory sequence since determination of trends and incremental effects resulting from parameter variations was the primary objective of the study.

---

<sup>1</sup>The word "booster" is used to refer to the initial thrusting stage of a complete satellite orbiting system.

## NOTATION

Symbols used in this study are defined as follows:

A	reference area, $\text{ft}^2$	
$C_D$	drag coefficient, $\frac{2D}{\rho V_E^2 A}$	
D	drag force, lb	
F	resultant force, lb	
$g$	gravitational acceleration, $\frac{\mu}{r^2}$ , $\text{ft/sec}^2$	A 5 2 1
h	altitude, ft, or nautical miles, as specified	
$I_{sp}$ , I	specific impulse, sec	
M	Mach number	
m	mass, slugs	
p	pressure, $\text{lb/ft}^2$	
R	radius of earth, ft or nautical miles	
r	radial distance from center of earth, $R + h$	
T	thrust, lb	
t	time, sec	
$t_b$	burning time, sec	
V	velocity, $\text{ft/sec}$	
W	weight, lb	
w	fuel weight flow, $\text{lb/sec}$	
$\beta$	heading, deg	
$\gamma$	flight-path angle, deg	
$\theta$	longitude, deg	
$\mu$	product of universal gravitational constant and mass of earth, $\text{ft}^3/\text{sec}^2$	

$\rho$  atmospheric density, slugs/cu ft  
 $\phi$  latitude, deg  
 $\omega$  rotational velocity of earth, radians/sec

## Subscripts

a local atmospheric conditions  
c circular orbit  
E earth (excludes earth's rotation)  
e engine exit, exhaust  
f fuel load  
g gross weight of stage, including payload  
h local horizontal  
o conditions at booster separation  
r radial (vertical) component  
p payload  
SL sea level  
st structure, inert weight  
T total  
1 first stage  
2 second stage  
 $\theta$  component normal to meridian  
 $\phi$  component tangent to meridian

## DESCRIPTION OF ROCKET VEHICLE

The vehicle used in this study was a payload package and a two-stage rocket with gross weight, stage weights, and specific impulse values representative of current technology. Specific values are given in tables I and II. In these tables and throughout this study, the stage numbering system, weights, weight ratios, payload ratios, and all other parameters refer to the vehicle after separation of the booster and do not include the booster. In the values of  $W_f$ ,  $W_{st}$ , and  $t_b$  given for stage 2 maximum burning time and therefore zero payload weight are assumed. These values will change as burning times change to meet the requirements of particular trajectories, and payload weight will change accordingly since it is assumed equal to the fuel weight remaining after the orbit has been established.

A  
5  
2  
1

## ANALYSIS

## Assumed Conditions

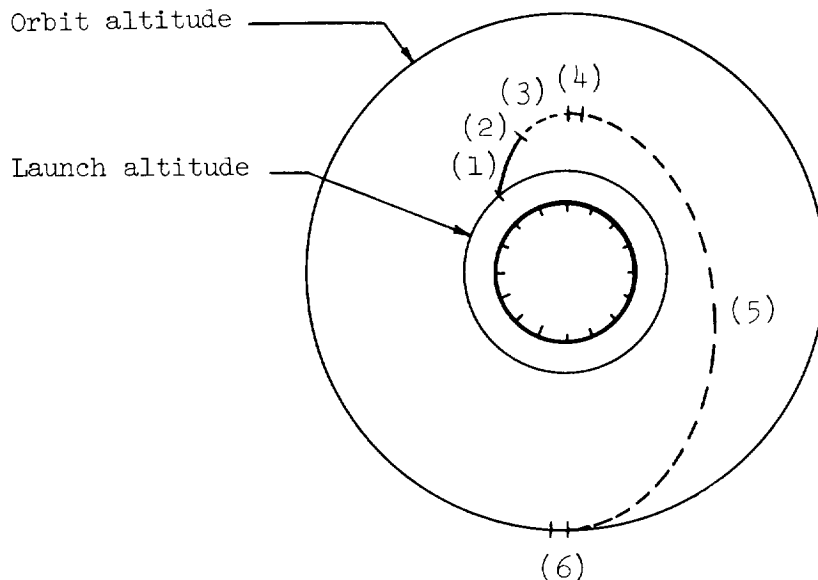
In this study, the equations of motion presented in the appendix and the conditions indicated were used to compute the trajectories. Since the trajectories were to be initiated at booster separation, the minimum altitude at separation being 90,000 feet, drag was considered sufficiently small to be unimportant to the results of the study and, therefore, was assumed zero. The trajectories were initiated at N 28.5° - W 81°, which is the vicinity of Cape Canaveral, with a heading of 90° (due east).

Payload ratio was computed with the assumption that the second stage was fuel and structure only, the weight of fuel remaining after injection being equal to the allowable payload weight for the initial conditions considered.

Trajectories used for the computations of this study are of two types and will be called (1) the Hohmann transfer ellipse trajectory and (2) the direct orbit trajectory.

## Trajectory Sequence

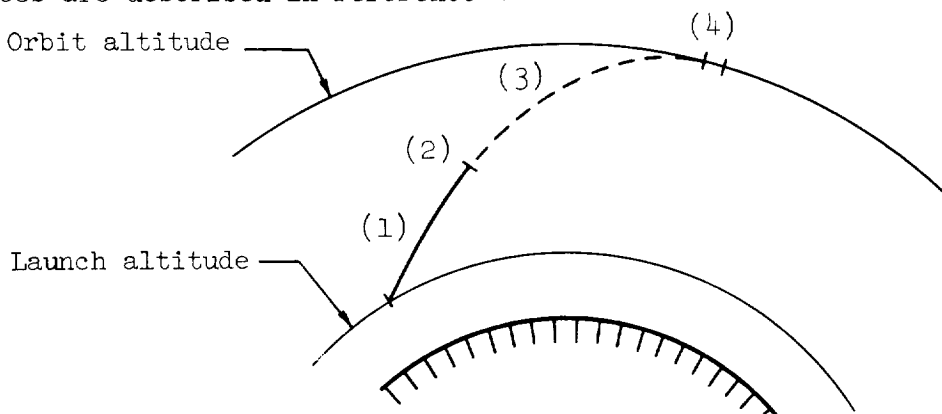
Hohmann transfer ellipse trajectory.- The sequence of this method, as shown in sketch (a), is (1) thrust until burnout of the first stage, (2) separation of first stage, (3) second stage coast to apogee of the trajectory where (4) a thrust impulse supplies the additional velocity required to reach a specific velocity, which is determined by the altitude. The point at which the required velocity is reached then becomes perigee.

A  
5  
2  
1

Sketch (a)

of an elliptical orbit path along which (5) the vehicle coasts to apogee where (6) a second thrust impulse (restart of second stage engine) circularizes the orbit. For this method the results of the analyses of transfer orbits presented in reference 3 were used.

Direct orbit trajectory.- The trajectory sequence of this method, as shown in sketch (b), was (1) thrust until burnout of the first stage, (2) separation of first stage, (3) second stage coasts until apogee of the trajectory is reached where (4) a thrust impulse brings the velocity up to that required for circular orbit. This and other trajectory sequences are described in reference 4.



Sketch (b)

Injection impulse.- In this study injection is accomplished at apogee of the initial trajectory with a thrust impulse so that no altitude losses occur. In actual conditions injection cannot be done impulsively but will require finite injection times. During this time an altitude loss will occur while the velocity is subcircular. Calculations indicate that this loss is not of sufficient magnitude to require special consideration except in some of the transfer ellipse trajectories with very low initial flight-path angles. These low angles allow apogee to be reached before burnout of the first stage so that injection into the transfer orbit is not possible. Although an injection impulse is used in this study, the requirement that burnout of the first stage must occur before apogee is reached limits the injection time. This also indicates the minimum angle which will meet this condition.

Vehicle parameters.- Thrust changes were obtained by varying fuel weight flow and engine exit reference area, with the specific impulse of the fuel being a constant value obtainable with existing fuels (table I). Because fuel load was fixed, burning times changed as fuel weight flow changed.

For the inert weight study of both trajectory methods, gross and stage weights of the vehicle (table II) were retained. Changes in inert weight were offset by comparable changes in fuel loads that resulted in changes in payload in orbit.

Orbit altitude.- The transfer ellipse trajectories were computed for an orbit altitude of 300 nautical miles (n.mi.). This altitude is well below the Van Allen radiation belts, yet is sufficiently high for long satellite lifetimes.

No specific orbit altitude was computed for the direct orbit trajectories, but a wide range of altitudes was considered.

#### RESULTS AND DISCUSSION

The results of this study are presented in figures 1 to 15. On these figures the ratio  $W_p/W_g$  refers to the final orbited payload divided by the gross weight of the vehicle after separation of the booster and does not include the weight of the booster. On figures 1 and 2 are the results of a brief study of initial altitude. Resulting payload ratios for the transfer ellipse trajectories are given for a range of initial flight-path angles and Mach numbers on figures 3 to 8, wherein figures 3, 5, and 7 are for constant first stage inert weight ratios and figures 4, 6, and 8 are for constant second stage inert weight ratios. The lower limits indicated on these figures are the estimated minimum angles to achieve the required apogee conditions stated previously. The upper limits indicate the angle at which the transfer ellipse trajectory

reduces to a direct orbit trajectory. At this angle the initial part of the trajectory sequence reaches the 300 n.mi. altitude without use of the transfer ellipse. Values of payload weight and flight-path angle for this limit are the same as those of the direct orbit method at 300 n.mi. for the same conditions. On figures 4, 6, and 8 the upper limit of flight-path angle increases as inert weight increases. This increase in flight-path angle results because with increase in inert weight, less fuel is available and therefore the burning time is shortened, and higher angles are necessary to reach 300 n.mi. The  $55^{\circ}$  angle was the maximum considered.

Because of the high thrust-weight ratios for low Mach numbers required for the low flight-path angles of the transfer ellipse method, the direct orbit method was studied to determine whether orbit conditions could be met with combinations of low  $T/W$  and  $M_0$ . On figures 9 to 14 results of computations made with this method show the payload ratio obtained for various flight-path angles, Mach numbers, inert weight ratios, and orbit altitudes. Constant first stage inert weight ratios are shown on figures 9, 11, and 13, and constant second stage inert weight ratios are shown in figures 10, 12, and 14. Except for the  $T/W = 2.5$  value at low inert weight ratios (figs. 13 and 14) the  $25^{\circ}$  angle did not allow an orbit altitude of 300 n.mi. to be reached with the maximum  $M_0 = 9$  considered; therefore  $25^{\circ}$  was the minimum angle used with this trajectory method. Since 75 to 100 n.mi. was felt to be the minimum practical altitude, the curves of these figures were terminated at altitudes in this range. Again  $55^{\circ}$  was the maximum angle considered.

Payload weight ratio values for the same vehicle computed with the two trajectory methods, are shown on figures 15(a) through 15(c). For these figures, the payload ratio value for minimum flight-path angle for a particular Mach number, taken from figures 3 to 8, form the ordinate. Payload ratio values at 300 n.mi. from figures 9 to 14 for the same Mach number form the abscissa.

#### Flight Conditions

Initial altitude.— Most of the computations were made with an initial altitude of 90,000 feet. To determine altitude effects several trajectories were computed with other altitudes and results for 350,000 feet are presented with the results for 90,000 feet on figures 1 and 2 for flight-path angles of  $35^{\circ}$  and  $45^{\circ}$ . For each angle, the orbit altitude change approximately equaled the initial altitude change and payload was nearly unchanged. Only the direct orbit trajectory could be used to check orbit altitude effects because the transfer ellipse trajectory must be computed for a predetermined orbit altitude.

Initial Mach number.- Results for both trajectory methods show increasing payload ratios as the Mach number is increased from 3 to 9 at any constant initial flight-path angle. The payload ratios increase because as the vehicle is boosted to higher velocity, its initial energy is increased. Thus more energy is expended from the booster, so less propulsive energy must be expended by the vehicle and more payload may be orbited.

Initial flight-path angle.- Results from both trajectory methods show that payload decreases as the flight-path angle increases. When the flight-path angle is large, most of the propulsive energy of the vehicle is expended in gaining altitude, leaving a large velocity increment to be made up during injection. This requires large amounts of fuel, allowing only small payloads. As the angle decreases, the propulsive energy provides more velocity at lower altitudes so injection must supply a smaller increment, allowing more payload. Thus the lowest angle that will give the required orbit will allow the highest payload for the initial conditions considered. Although initial flight-path angles from  $6^\circ$  to  $55^\circ$  were considered,  $10^\circ$  was the lowest angle that could be used with the transfer ellipse trajectories. As stated previously,  $25^\circ$  was the lowest angle used with the direct orbit trajectories.

Thrust-weight ratio.- When fuel load is fixed but fuel flow rate is increased to increase thrust, shorter burning times result. A higher value of  $T/W$  does give more velocity at burnout of the first stage, but burnout occurs at larger flight-path angles because of the shorter burning time and requires longer coasting periods to reach apogee. When the vehicle does reach apogee after the long coast period, it has little more velocity than it had when lower values of  $T/W$  were used. Injection must supply approximately the same velocity increment for each condition, so resulting payloads are nearly equal. This is evident on figures 3 to 8 for the transfer ellipse method where the main effect of increases in  $T/W$  is to decrease both the upper and lower limits of the flight-path angle. For the direct orbit trajectories (figs. 9 to 14), changes in  $T/W$  plus the influence of other parameters change the payload. The two most apparent conditions are: (1) when orbit altitude and initial Mach number are fixed, payload increases with  $T/W$  because smaller initial angles can be used to reach that altitude; (2) when initial angle and Mach number are fixed, payload decreases with increasing  $T/W$  because orbit altitude is higher. Payload change is small in either condition.

Trajectory method.- Payload weight ratios resulting from the two trajectory methods for the same values of  $M_0$ ,  $h_0$ ,  $T/W$ , and orbit altitude (figs. 15(a) to 15(c)) show the linear variation of payload weight ratios that occurs with changes in initial conditions.

A  
5  
2  
1

## CONCLUDING REMARKS

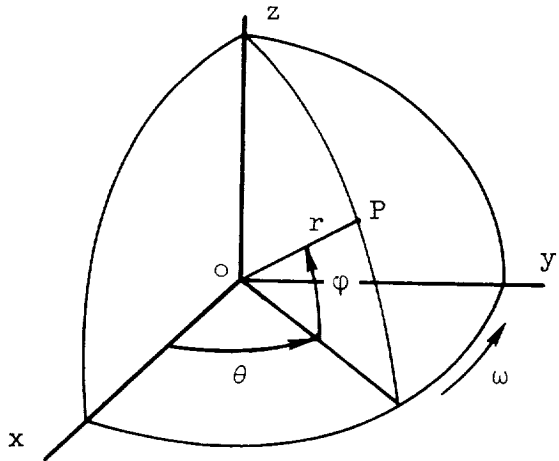
An analysis of conditions at booster separation involving variations in Mach number, flight-path angle, altitude, thrust, and inert weight has been made for a two-stage rocket which forms the upper stages of a satellite launching vehicle. Many combinations of these parameters gave the desired 300 nautical mile orbit altitude, but also desired was the maximum payload weight at this altitude for the trajectories that were used. With either the transfer ellipse or the direct orbit trajectory, the payload weight was highest for low initial flight-path angles and high initial Mach numbers. Of course, high initial Mach numbers require greater energy expenditures from the booster. Changes in initial altitude had little effect on payload weight. For a particular orbit altitude, small gains in payload weight occurred when thrust-weight ratio was increased and smaller initial angles could be used to reach that altitude.

Ames Research Center  
National Aeronautics and Space Administration  
Moffett Field, Calif., July 6, 1961

## APPENDIX

## EQUATIONS OF MOTION

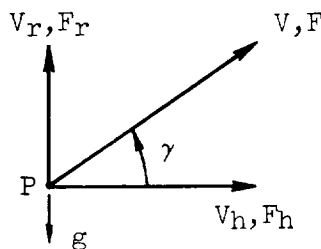
Computations for this study were made on an IBM-704 digital computer. The equations used were written for an assumed homogeneous, spherical, rotating earth; inverse square gravitational field; 1956 ARDC atmosphere (ref. 5); and gravity turn trajectories. With the aid of the accompanying sketches, a brief derivation of the equations of motion follows:



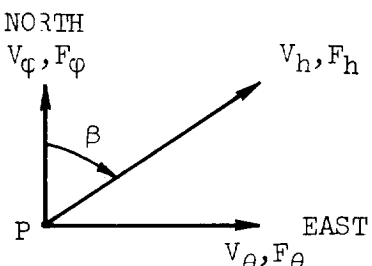
Sketch (c).- Three-dimensional earth axes.

ox,oy,oz	coordinates fixed in earth
oxy	equatorial plane
oz	polar axis
$\theta$	longitude
$\phi$	latitude
r	$R + h$ , $R$ = radius of earth $h$ = altitude
$\omega$	earth rotational velocity

A  
5  
2  
1



Sketch (d).- Horizontal and vertical components of force and velocity at point P;  $\gamma$  = flight-path angle, deg.



Sketch (e).- Components of horizontal force and velocity at point P;  $\beta$  = heading, deg.

The horizontal and vertical components of force and velocity, sketch (d), are:

$$V_h = V \cos \gamma$$

$$V_r = \dot{r} = V \sin \gamma$$

$$F_h = F \cos \gamma$$

$$F_r = F \sin \gamma - mg$$

Components of force and velocity in the horizontal plane, and their relation to the earth axes, sketches (c) and (e), are:

$$V_h \sin \beta = (r \cos \varphi)(\dot{\theta} + \omega) = V_\theta$$

$$V_h \cos \beta = r\dot{\varphi} = V_\varphi$$

$$F_h \sin \beta = F_\theta$$

$$F_h \cos \beta = F_\varphi$$

The motion equations are derived as follows from Lagrange's equation:

$$\frac{d}{dt} \left( \frac{\partial T'}{\partial \dot{q}_i} \right) - \frac{\partial T'}{\partial q_i} = F_i$$

where

$$T' = \text{kinetic energy} = 1/2 mV^2$$

$$V^2 = \dot{r}^2 + r^2\dot{\varphi}^2 + (r^2 \cos^2 \varphi)(\dot{\theta} + \omega)^2$$

$q_i$  = system coordinates  $r, \theta, \varphi$

$F_i$  = generalized force along the  $q_i$  coordinate

Differentiating and combining terms gives the initial form of the motion equations

$$(1) m[\ddot{r} - r\dot{\varphi}^2 - r(\dot{\theta} + \omega)^2 \cos^2 \varphi] = F_r$$

$$(2) m[2r\dot{r}\dot{\varphi} + r^2\ddot{\varphi} + r^2(\dot{\theta} + \omega)^2 \sin \varphi \cos \varphi] = rF_\varphi$$

$$(3) m[2r\dot{r} \cos^2 \varphi (\dot{\theta} + \omega) - 2r^2 \sin \varphi \cos \varphi \dot{\varphi}(\dot{\theta} + \omega)$$

$$+ (r \cos \varphi)^2 \ddot{\theta}] = r \cos \varphi F_\theta$$

The force equations, which have been derived previously, are repeated and rearranged to give:

$$(4) F_r = -gm + F \sin \gamma$$

$$(5) F_\phi = F_h \cos \beta = F \cos \gamma \cos \beta$$

$$(6) F_\theta = F_h \sin \beta = F \cos \gamma \sin \beta$$

where  $F = T - D$ ;  $D = (1/2)\rho C_D V_E^2 A$ ;  $g = \mu/r^2$ ;  $D = 0$  for this study.

The final forms for these equations are:

$$(1) \ddot{r} = \frac{F_r}{m} + r\dot{\phi}^2 + r \cos^2 \phi (\dot{\theta} + \omega)^2$$

$$(2) \ddot{\phi} = \frac{(F_\phi/m) - 2\dot{r}\dot{\phi}}{r} - (\dot{\theta} + \omega)^2 \cos \phi \sin \phi$$

$$(3) \ddot{\theta} = \frac{(F_\theta/m) - 2(\dot{\theta} + \omega)(\dot{r} \cos \phi - r\dot{\phi} \sin \phi)}{r \cos \phi}$$

$$(4) \frac{F_r}{m} = -\frac{\mu}{r^2} + \left( \frac{T}{m} - \frac{1}{2} \rho \frac{C_D A}{m} V_E^2 \right) \sin \gamma$$

$$(5) \frac{F_\phi}{m} = \left( \frac{T}{m} - \frac{1}{2} \rho \frac{C_D A}{m} V_E^2 \right) \cos \beta \cos \gamma$$

$$(6) \frac{F_\theta}{m} = \left( \frac{T}{m} - \frac{1}{2} \rho \frac{C_D A}{m} V_E^2 \right) \sin \beta \cos \gamma$$

Constants in these equations are:

$$\mu = 1.40775 \times 10^{16} \text{ ft}^3/\text{sec}^2$$

$$\omega = 7.2921158 \times 10^{-5} \text{ radians/sec (at equator)}$$

$$R = 20,926,428 \text{ ft}$$

Thrust variation with altitude was included according to the equation

$$T_{\text{total}} = T + \Delta T = \frac{w}{g} V_e + A_e (F_e - p_a)$$

where

$w$  fuel flow rate, lb/sec

$V_e$  exhaust velocity, ft/sec

A  
5  
2  
1

$p_e$  exhaust pressure,  $\text{lb}/\text{ft}^2$ , assumed equal to sea-level pressure

$p_a$  local atmospheric pressure,  $\text{lb}/\text{ft}^2$

$A_e$  exhaust reference area,  $\text{ft}^2$

Design of the engine is such that the first term of this equation is considered constant for all altitudes above the design altitude; therefore, thrust will change with altitude in accordance with the pressure difference in the second term.

A  
5  
2  
1  
The equation used to determine the amount of fuel needed to add the required velocity during injection is:

$$\Delta V = I g_{SL} \ln \frac{W}{W - W_f}$$

or

$$W_f = W \left( 1 - e^{-\Delta V / I g_{SL}} \right)$$

where

$W$  vehicle weight before injection

$W_f$  weight of fuel

$I$  specific impulse

$g_{SL}$  gravity at sea level

$\Delta V$  additional velocity required

## REFERENCES

1. Buschmann, R. P.: Recoverable Boosters - The Next Big Step in Satellite and Space Systems. ARS Paper No. 1012-59, Nov. 1959.
2. Lysdale, C. A.: Launch-Vehicle Recovery Techniques. IAS Paper No. 61-51, Jan. 1961.
3. Wolaver, Lynn E.: A Study of the Satellite Equations of Motion and Transfer Orbits. WADC TN 58-378, Dec. 1958.
4. Keller, Charles L.: Satellite Ascent Paths. Sperry Engineering Review, vol. 11, no. 4, Dec. 1958, pp. 2-14.
5. Minzner, R. A., and Ripley, W. S.: ARDC Model Atmosphere 1956. ASTIA Document 110233, no. 86, 1956.

A  
5  
2  
1

TABLE I.- VEHICLE PERFORMANCE PARAMETERS

Stage	T/W	T	I <sub>sp</sub>	w	A <sub>e</sub>	t <sub>b</sub> at W <sub>st</sub> /W <sub>o</sub> = 0.05	t <sub>b</sub> at W <sub>st</sub> /W <sub>o</sub> = 0.15
1	1.5	346500	289	1198.96	22	140.36	125.58
1	2.0	462000	289	1598.62	29.3	105.27	94.19
1	2.5	577500	289	1998.27	36.6	84.21	75.35
2	1.5	80790	289	279.55	15	183.03	163.77
2	2.0	107720	289	372.73	20	137.28	122.83
2	2.5	134650	289	465.92	25	109.82	98.26

TABLE II.- VEHICLE WEIGHTS

Stage	W <sub>st</sub> /W <sub>o</sub>	W <sub>g</sub>	W <sub>o</sub>	W <sub>f</sub> <sub>max</sub>	W <sub>st</sub>	W <sub>p</sub>
1	0.05	231000	177140	168283	8857	53860
1	.15	231000	177140	150569	26571	53860
2	.05	53860	53860	51167	2693	0
2	.15	53860	53860	45781	8079	0



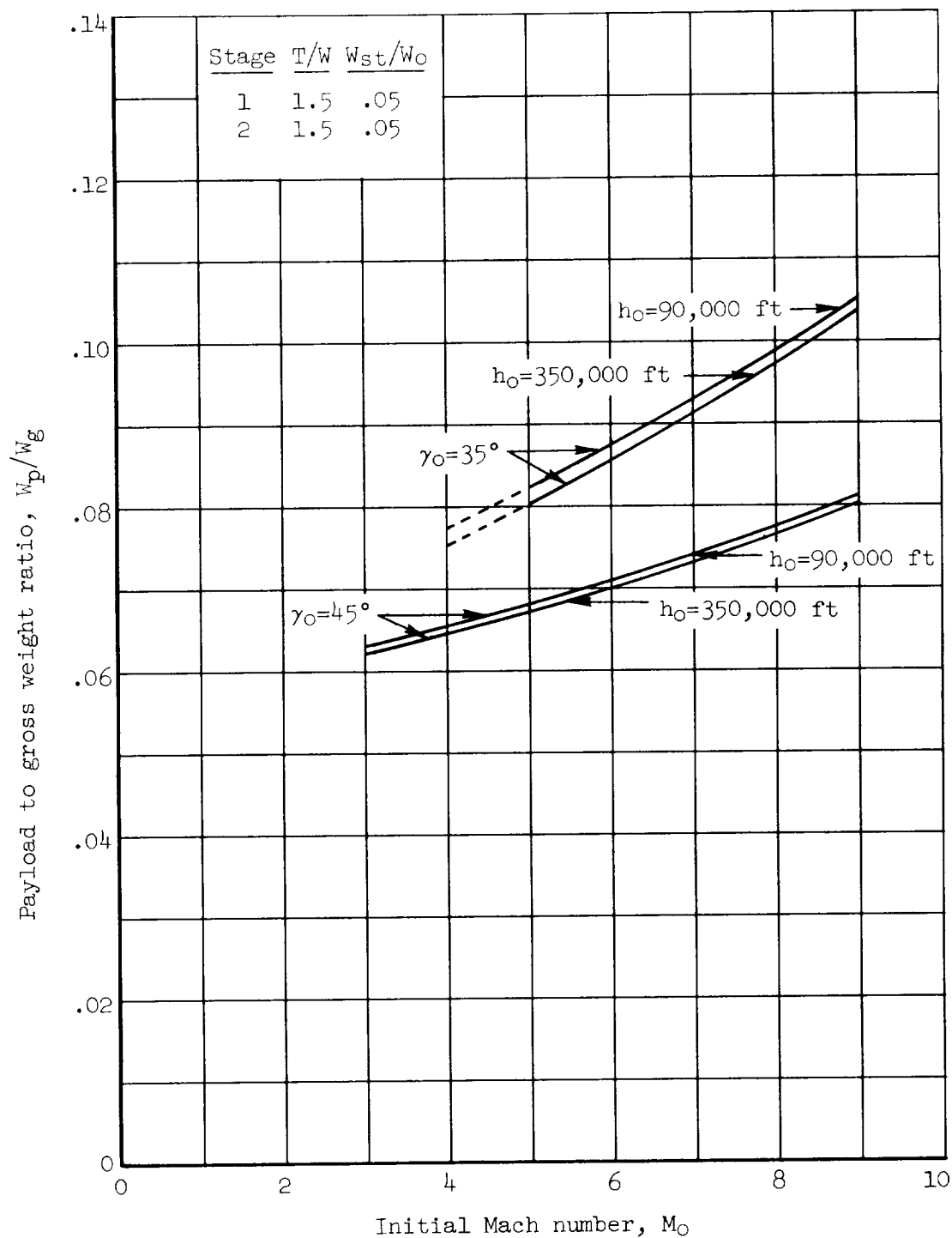


Figure 1.- Effect of initial altitude on payload weight ratio.

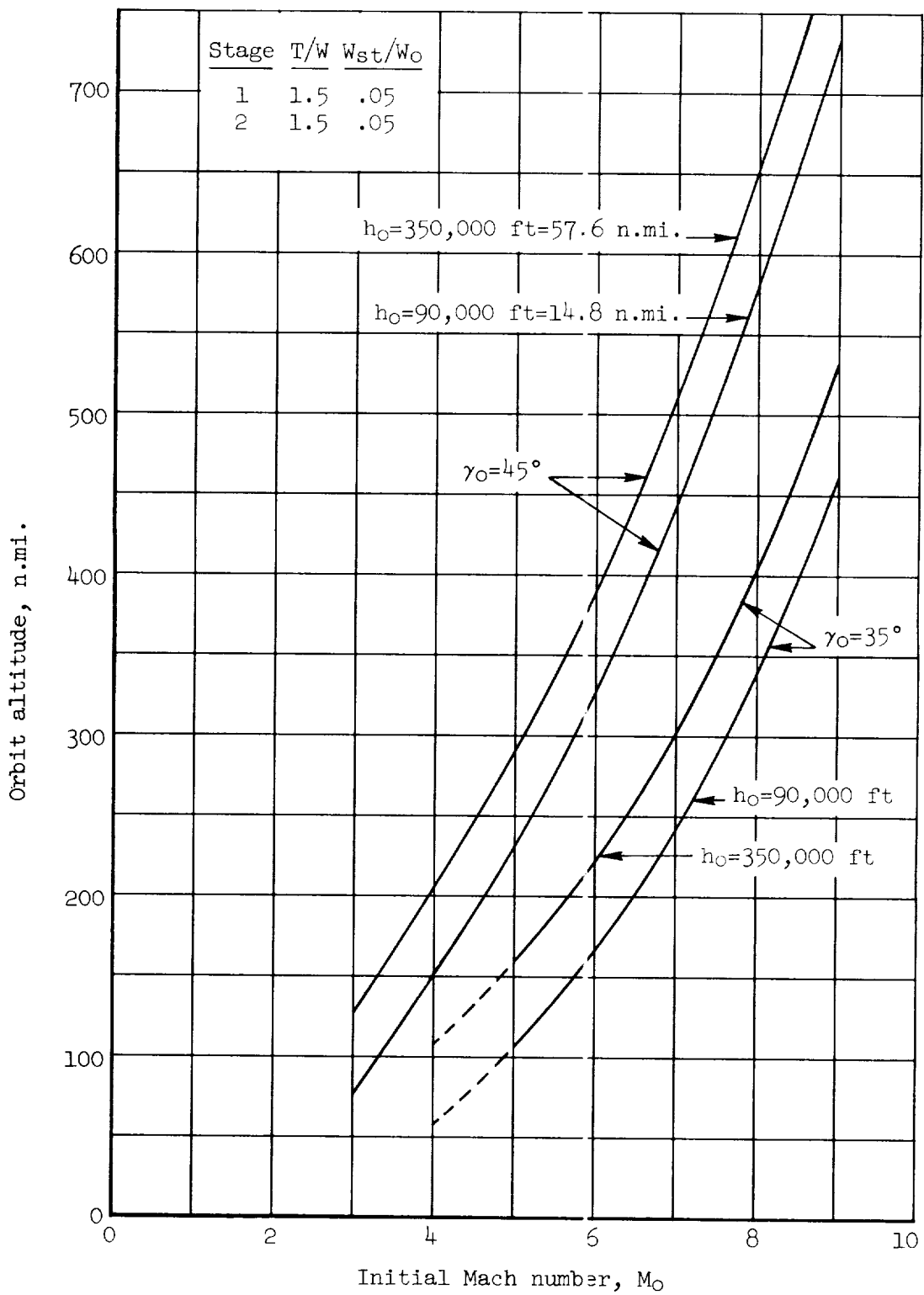


Figure 2.- Effect of initial altitude on orbit altitude.

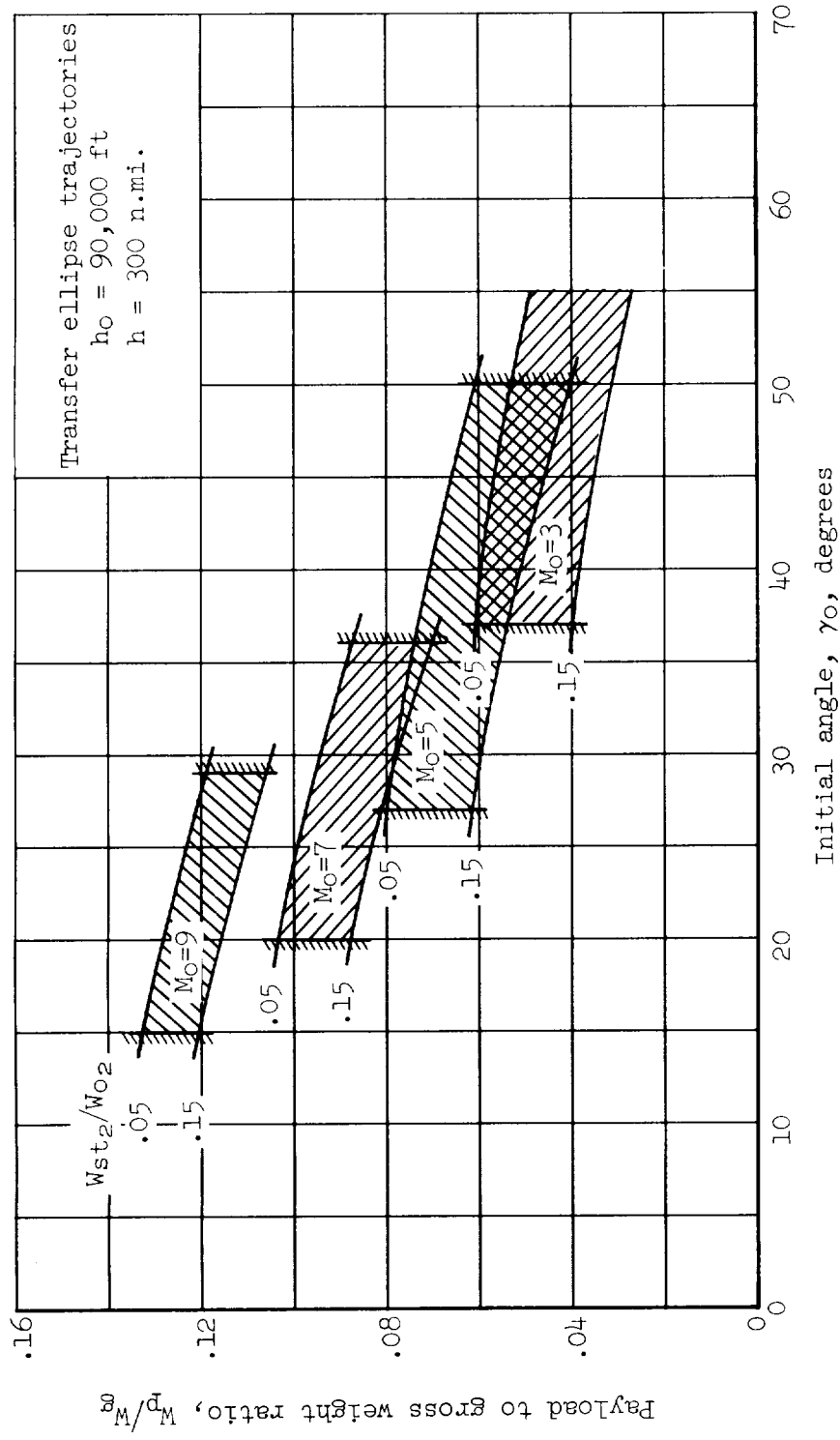
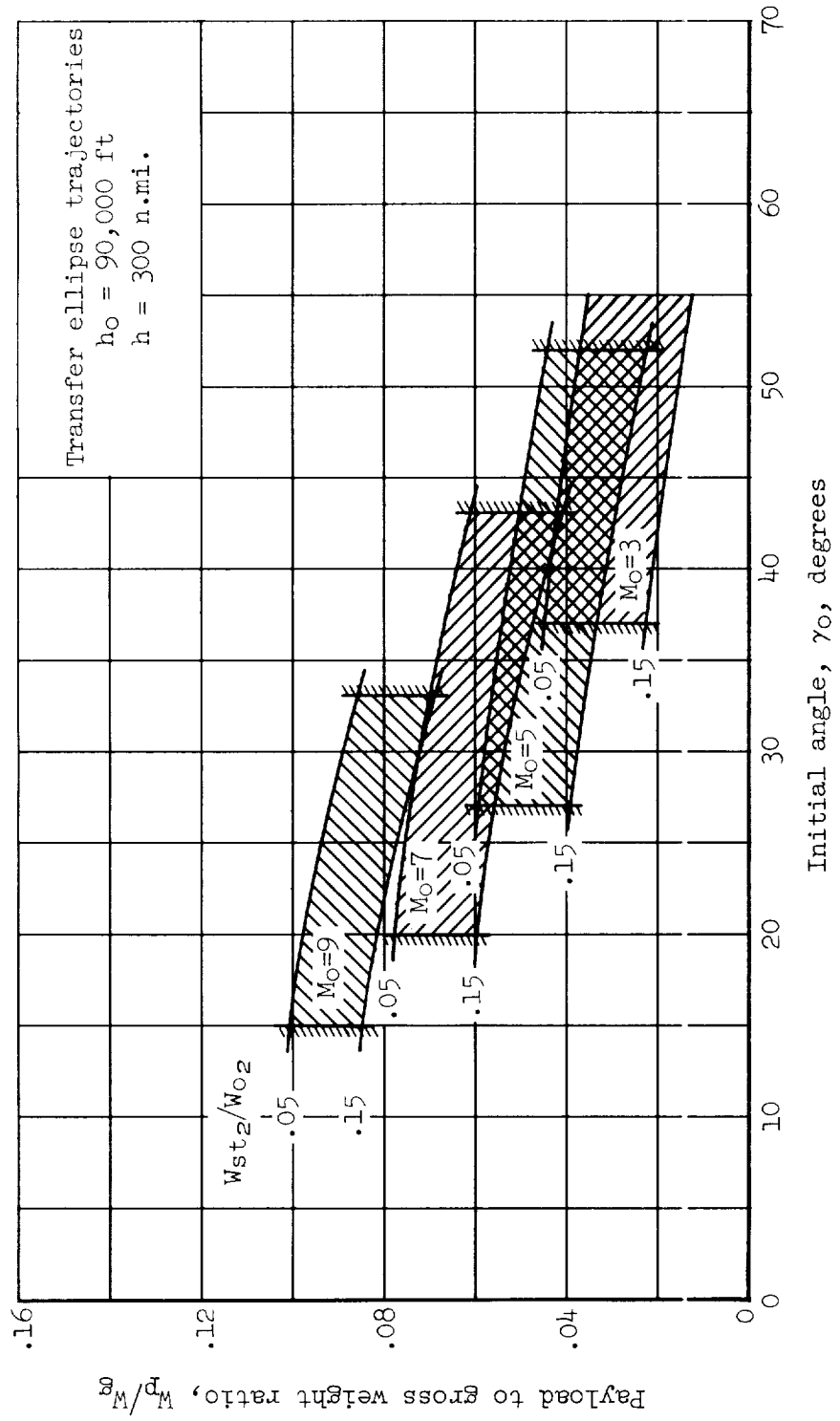


Figure 3.- Effect of initial angle, Mach number and second stage inert weight ratio on payload ratio for  $T/W = 1.50$ .

(a) First stage inert weight ratio,  $W_{st1}/W_{01} = 0.05$



(b) First stage inert weight ratio,  $W_{st_1}/W_{O_1} = 0.15$

Figure 3.- Concluded.

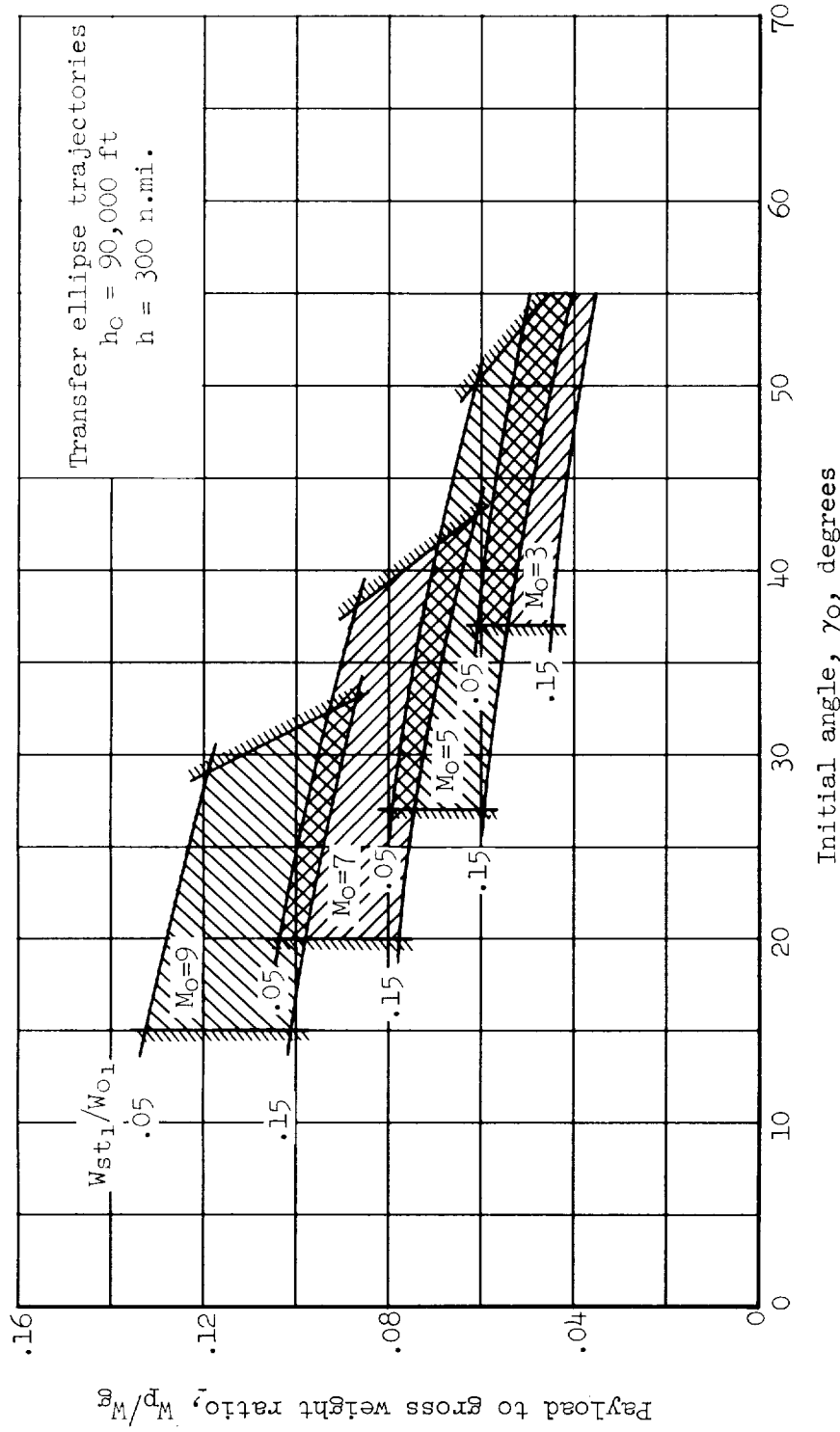
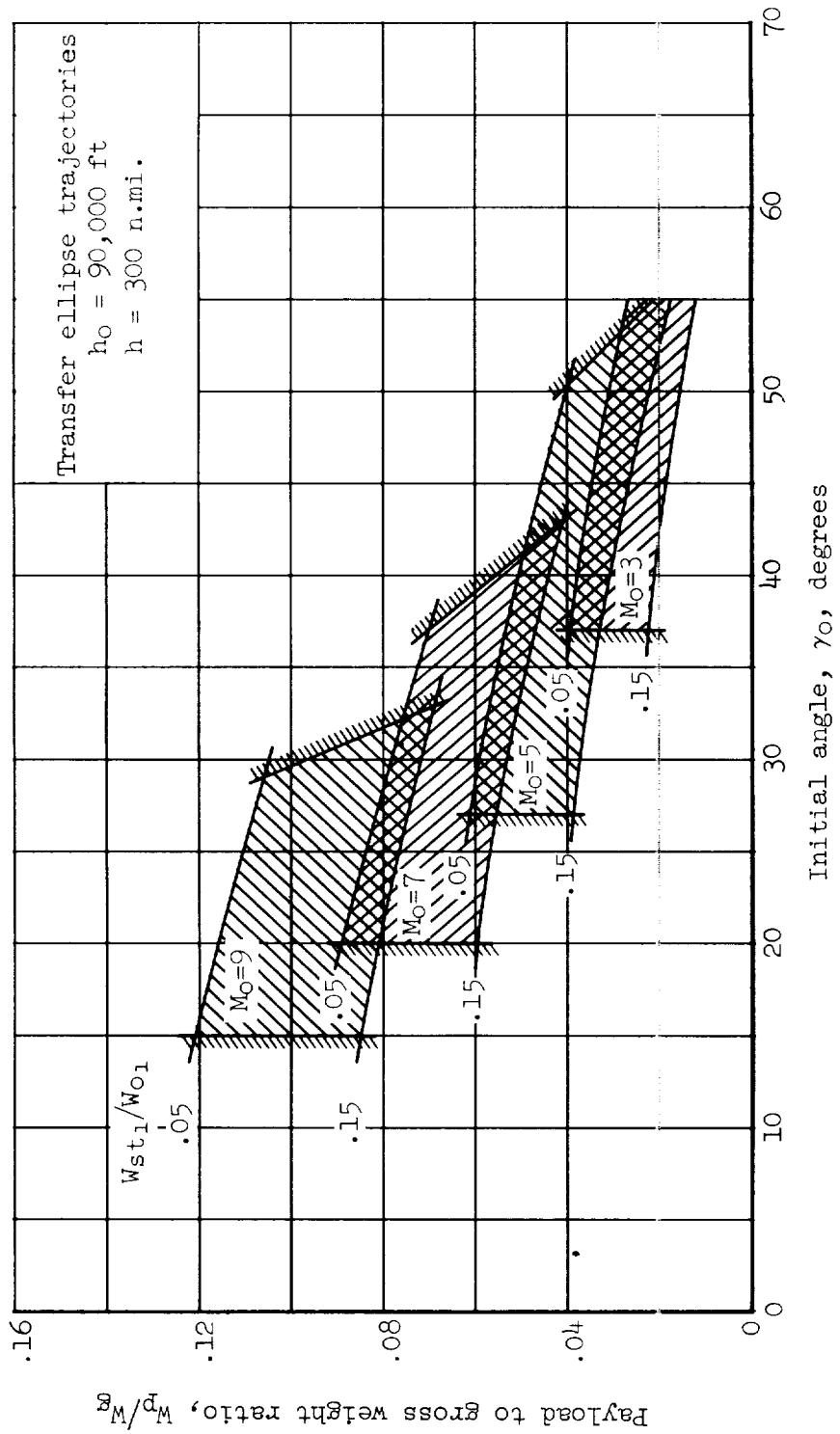
(a) Second stage inert weight ratio,  $W_{st_2}/W_{o_2} = 0.05$ 

Figure 4.- Effect of initial angle, Mach number and first stage inert weight ratio on payload ratio for  $T/W = 1.50$ .



(b) Second stage inert weight ratio,  $W_{st2}/W_{o2} = 0.15$

Figure 4.- Concluded.

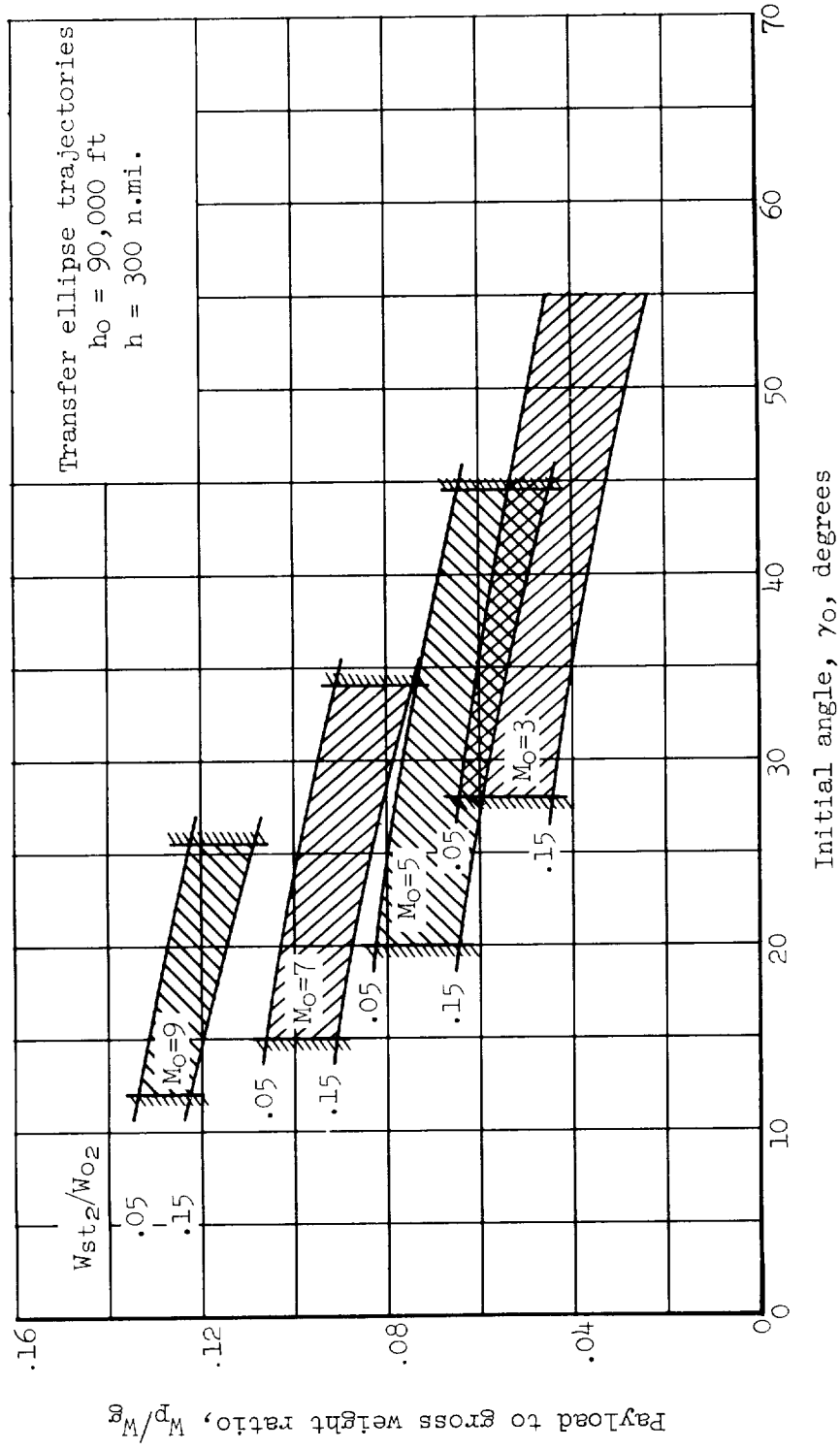
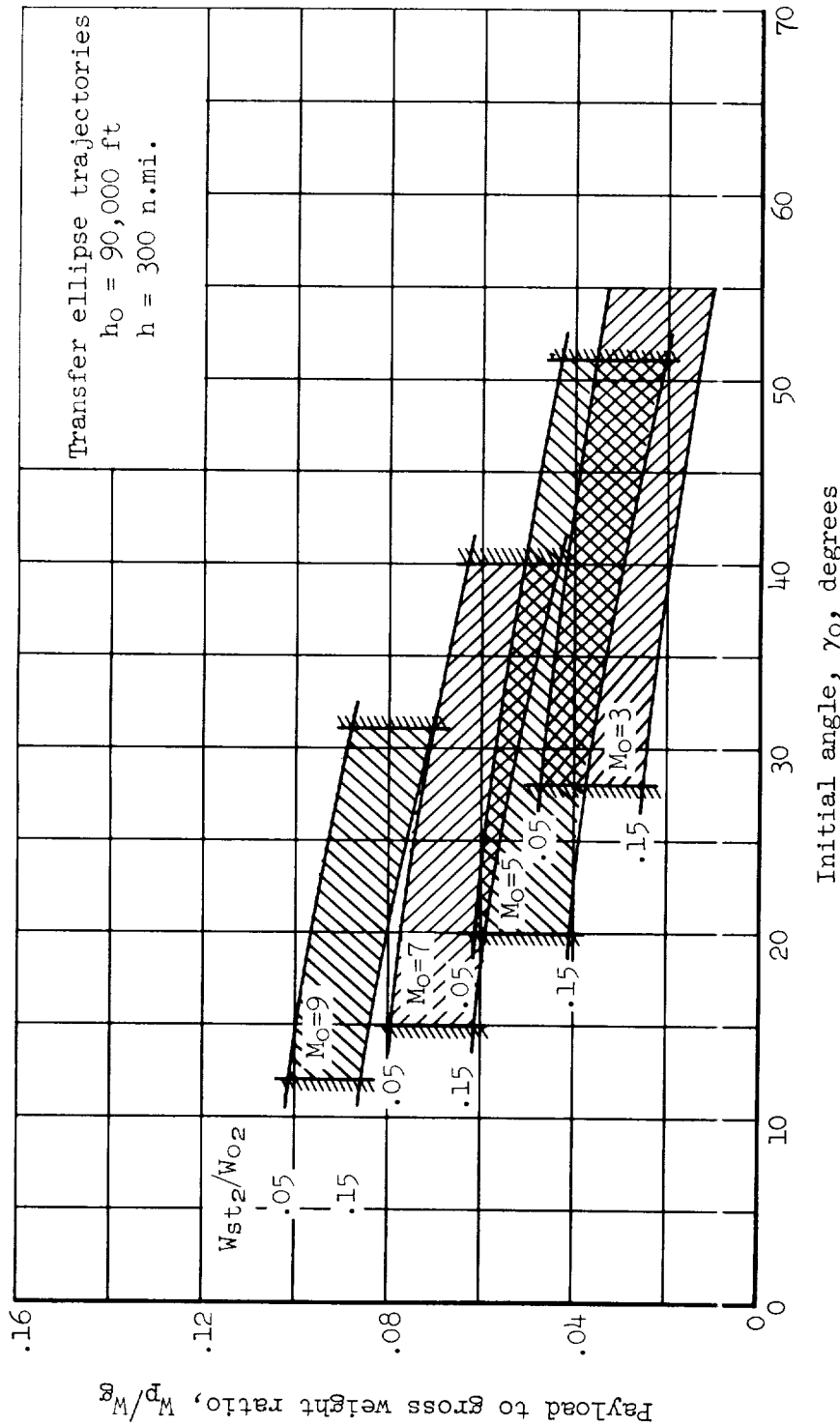
(a) First stage inert weight ratio,  $W_{st1}/W_{o1} = 0.05$ 

Figure 5.- Effect of initial angle, Mach number and second stage inert weight ratio on payload ratio for  $T/W = 2.00$ .



(b) First stage inert weight ratio,  $W_{st1}/W_{01} = 0.15$

Figure 5.- Concluded.

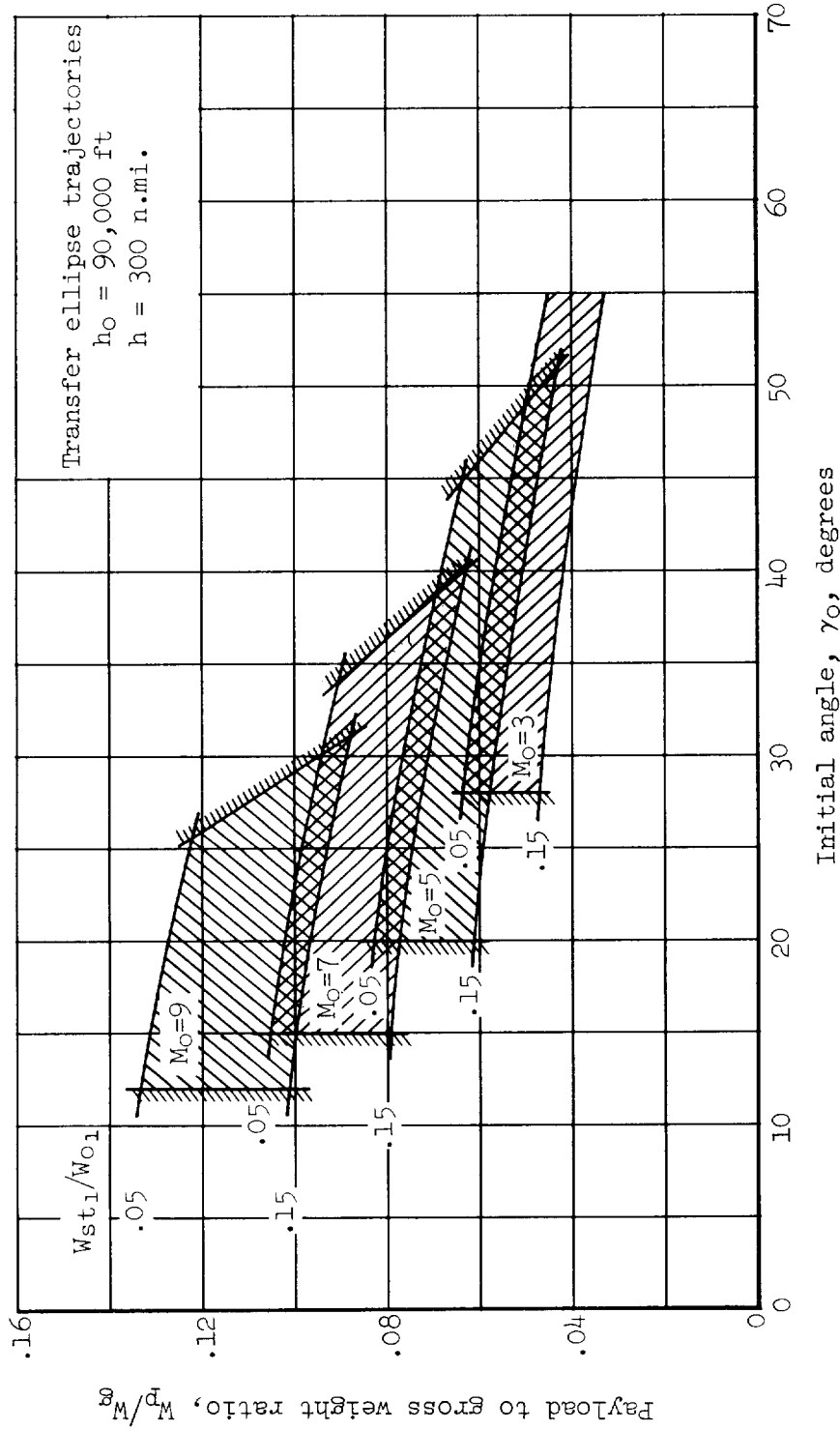
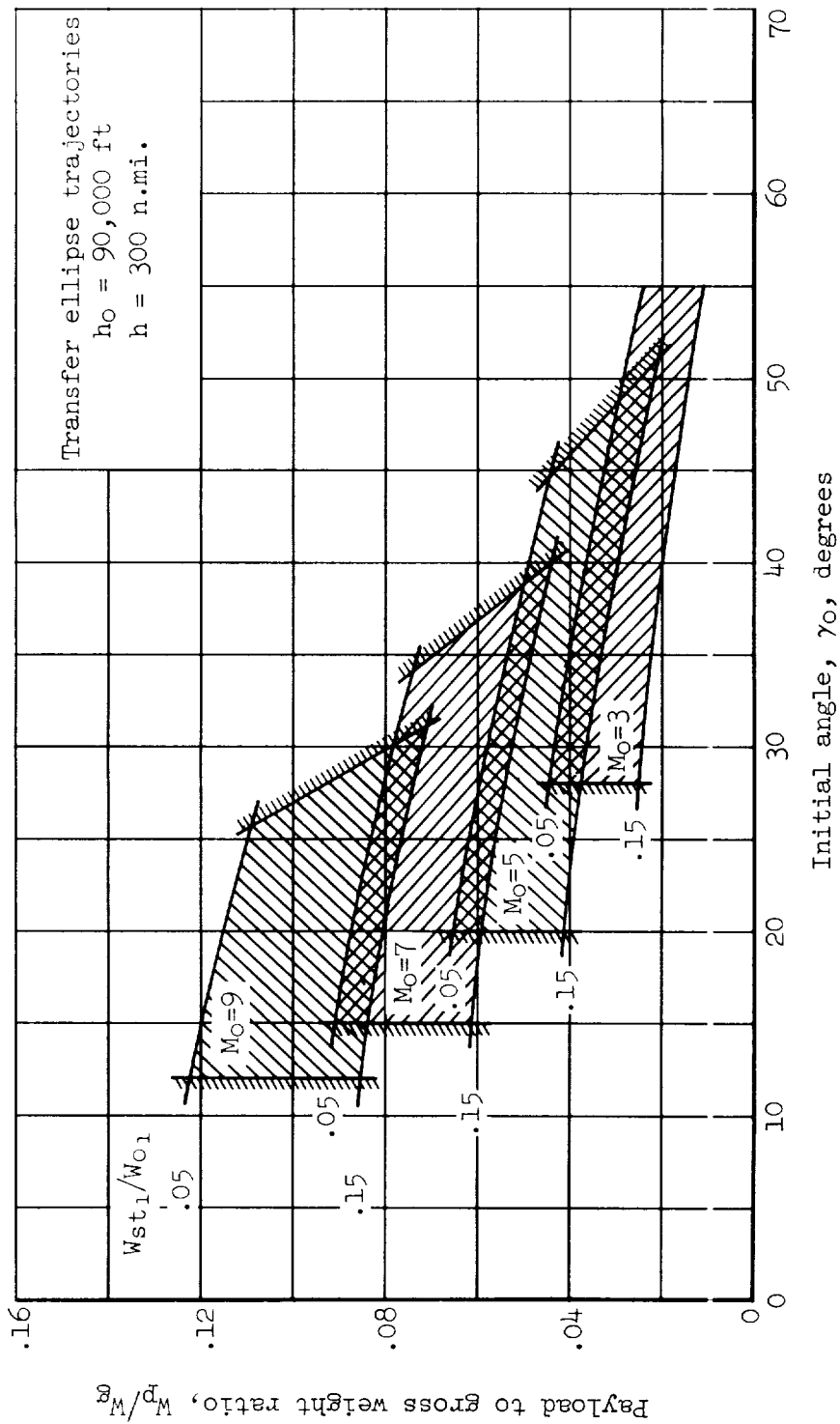
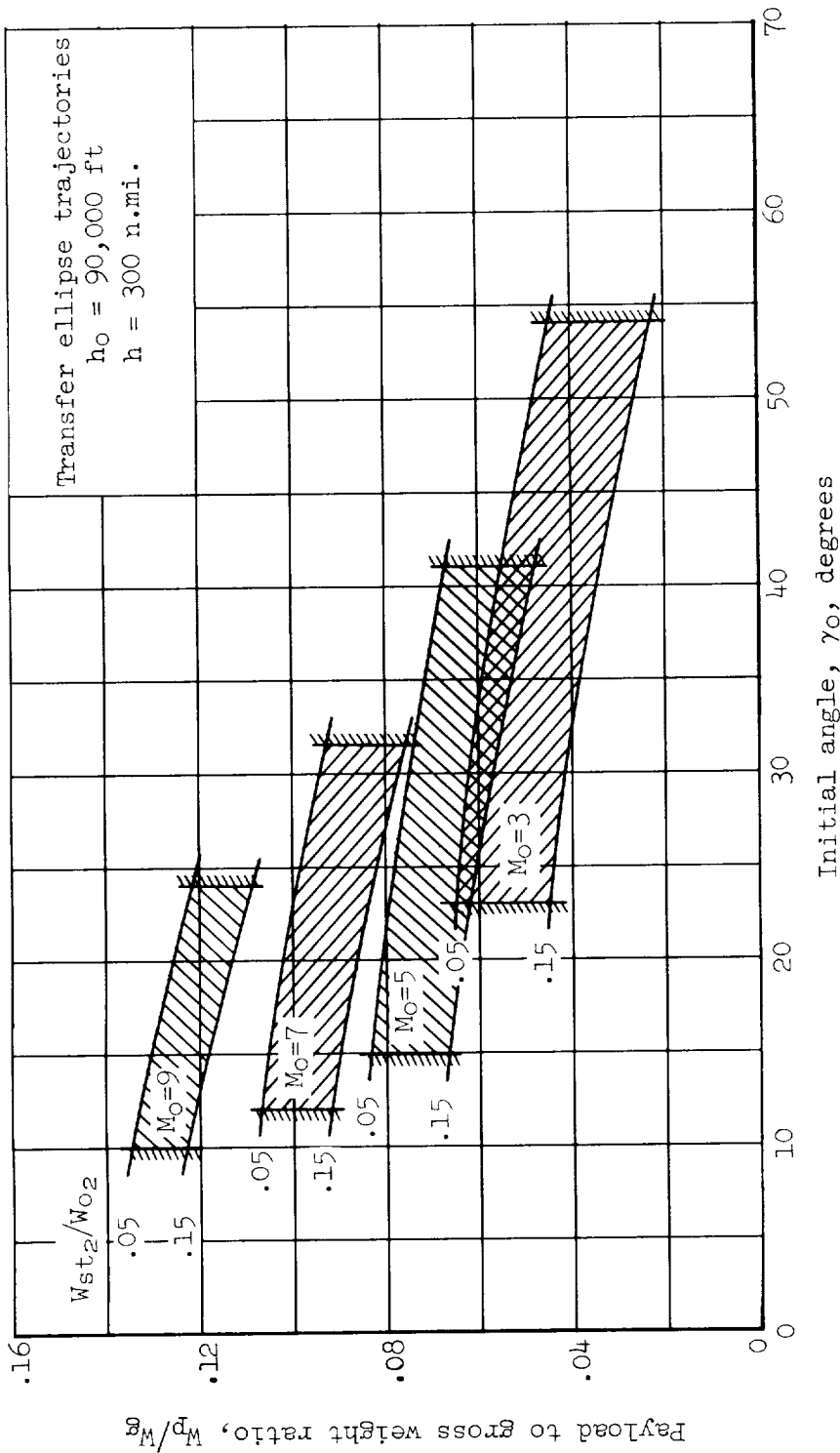
(a) Second stage inert weight ratio,  $W_{st2}/W_{02} = 0.05$ 

Figure 6.- Effect of initial angle, Mach number and first stage inert weight ratio on payload ratio for  $T/W = 2.00$ .



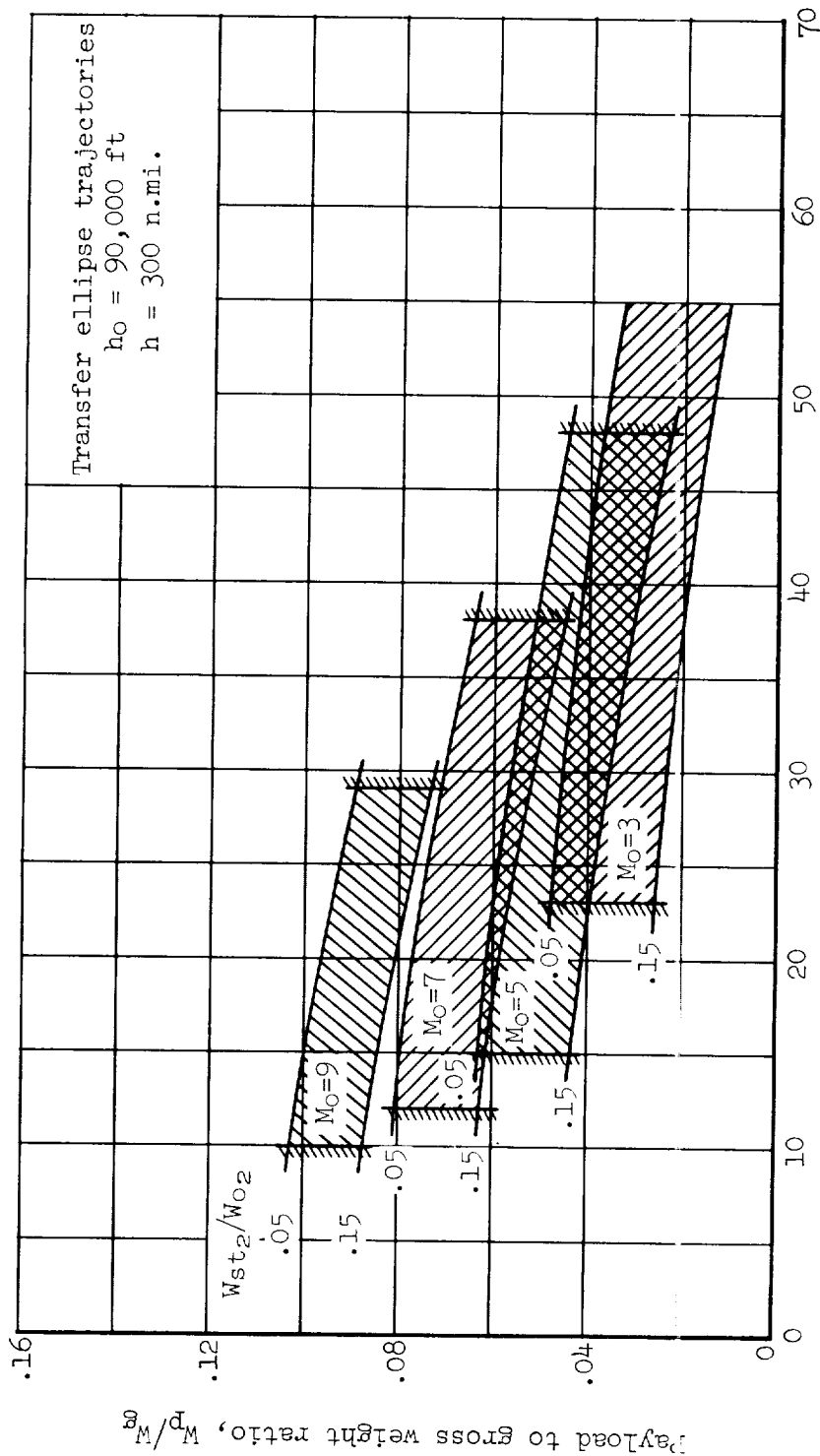
(b) Second stage inert weight ratio,  $W_{st2}/W_{o2} = 0.15$

Figure 6.- Concluded.



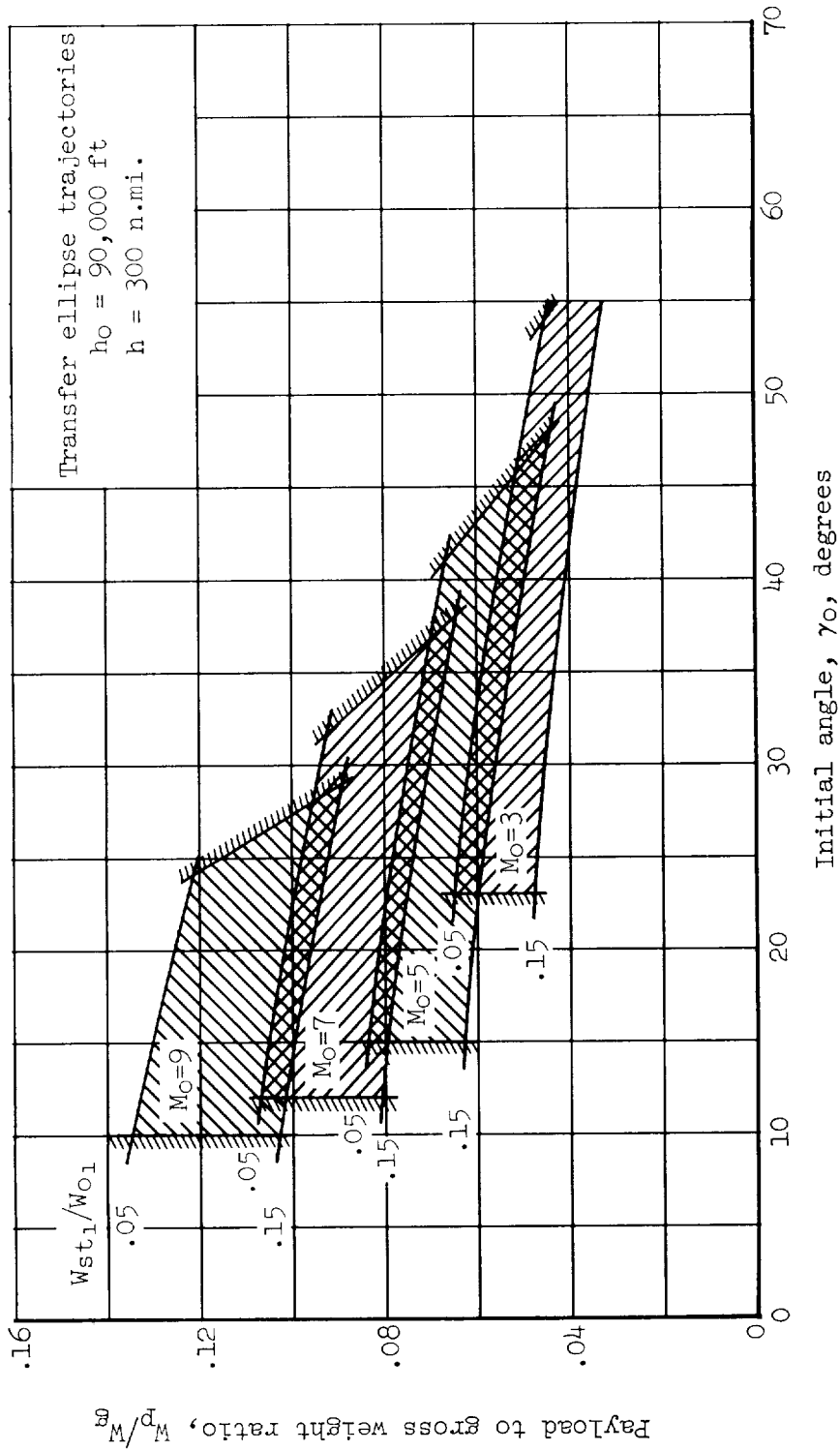
(a) First stage inert weight ratio,  $W_{st1}/W_{01} = 0.05$

Figure 7.- Effect of initial angle, Mach number and second stage inert weight ratio on payload ratio for  $T/W = 2.50$ .

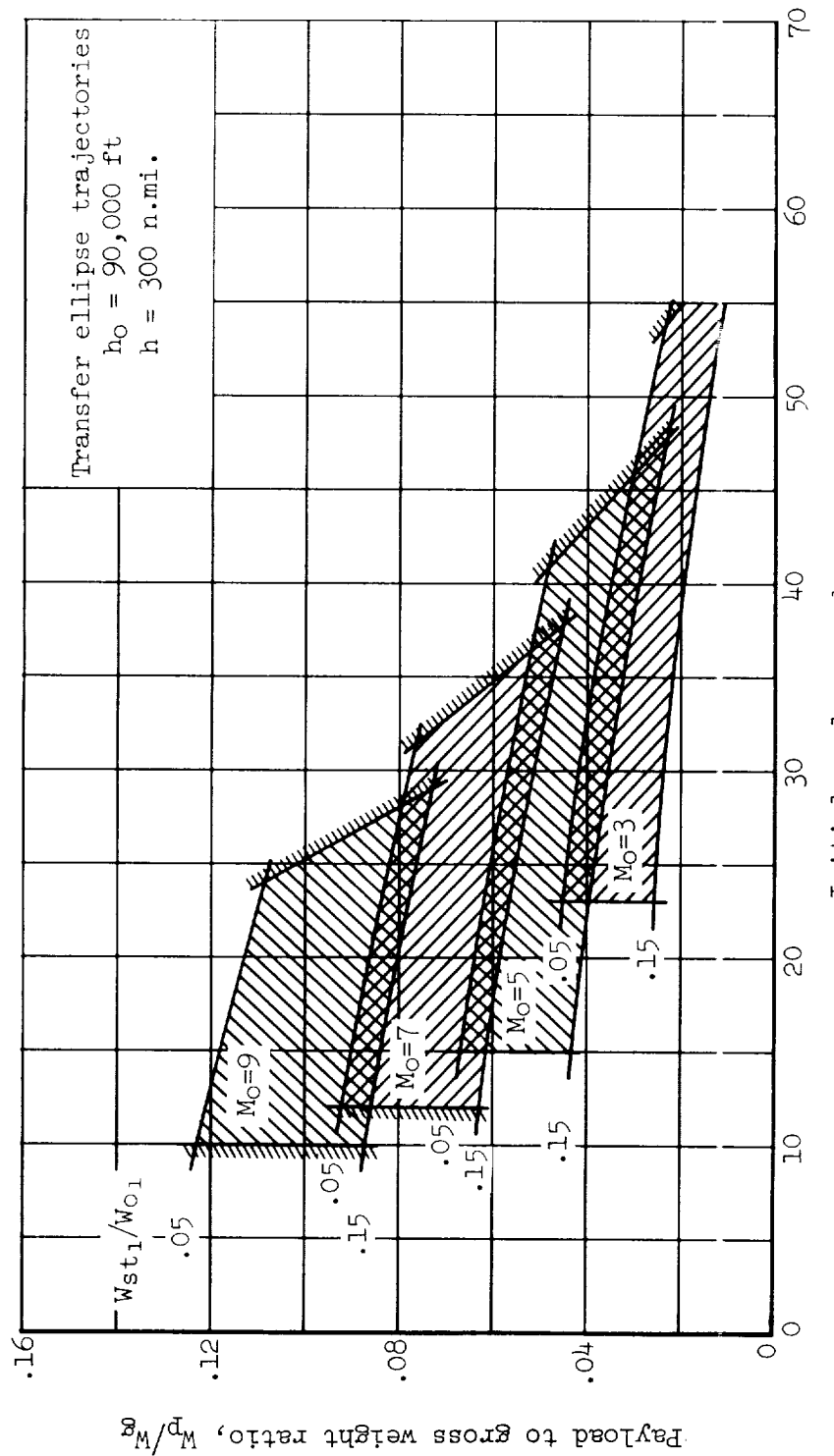


(b) First stage inert weight ratio,  $W_{st1}/W_{o1} = 0.15$

Figure 7.- Concluded.



(a) Second stage inert weight ratio,  $W_{st2}/W_{o2} = 0.05$   
 Figure 8.- Effect of initial angle, Mach number and first stage inert weight ratio on payload ratio for  $T/W = 2.50$ .



(b) Second stage inert weight ratio,  $W_{st2}/W_{02} = 0.15$

Figure 8.- Concluded.

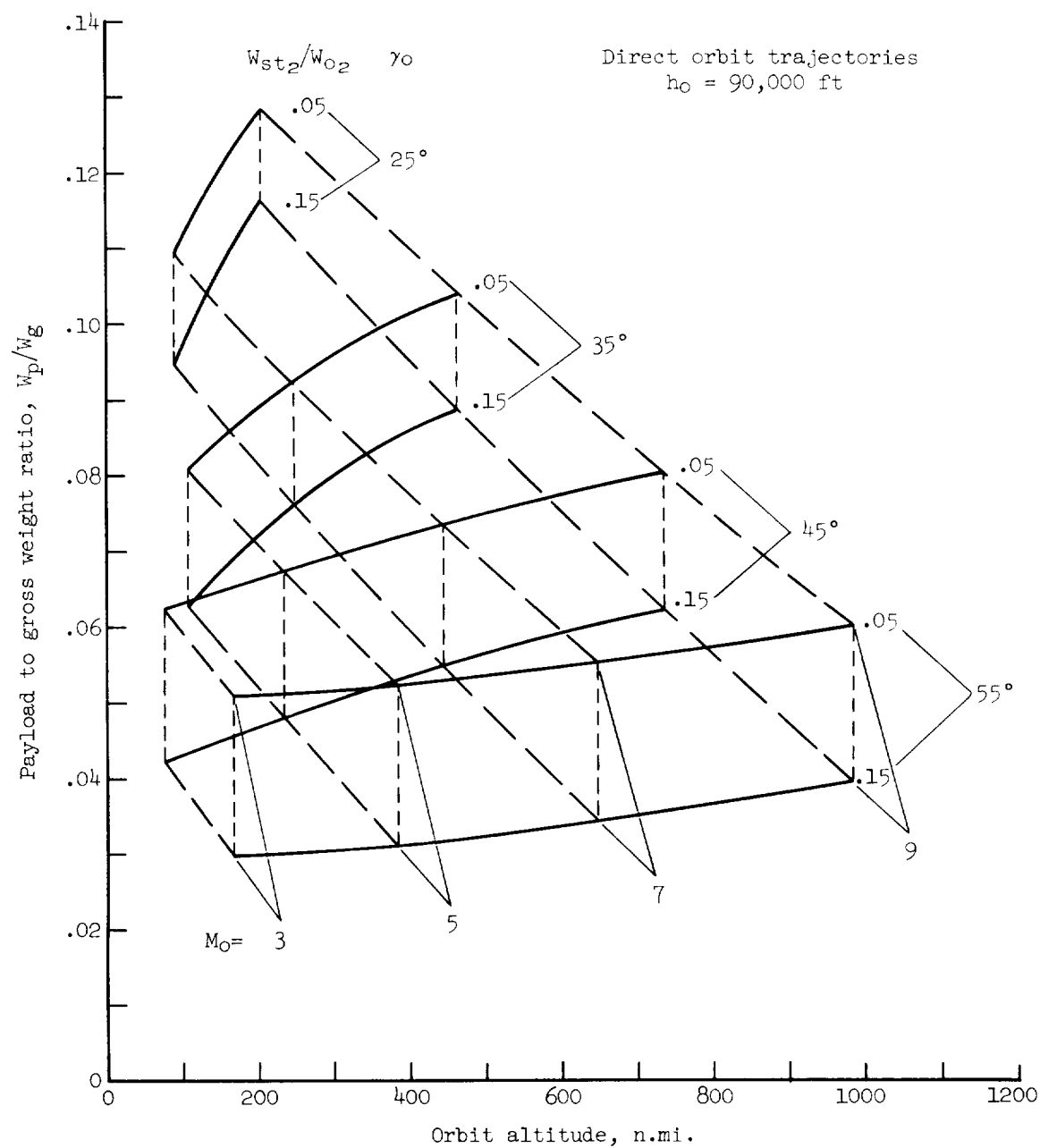
A  
5  
2  
1(a) First stage inert weight ratio,  $W_{st1}/W_{o1} = 0.05$ 

Figure 9.- Effect of initial angle, Mach number, orbit altitude and second stage inert weight ratio on payload ratio for  $T/W = 1.50$ .

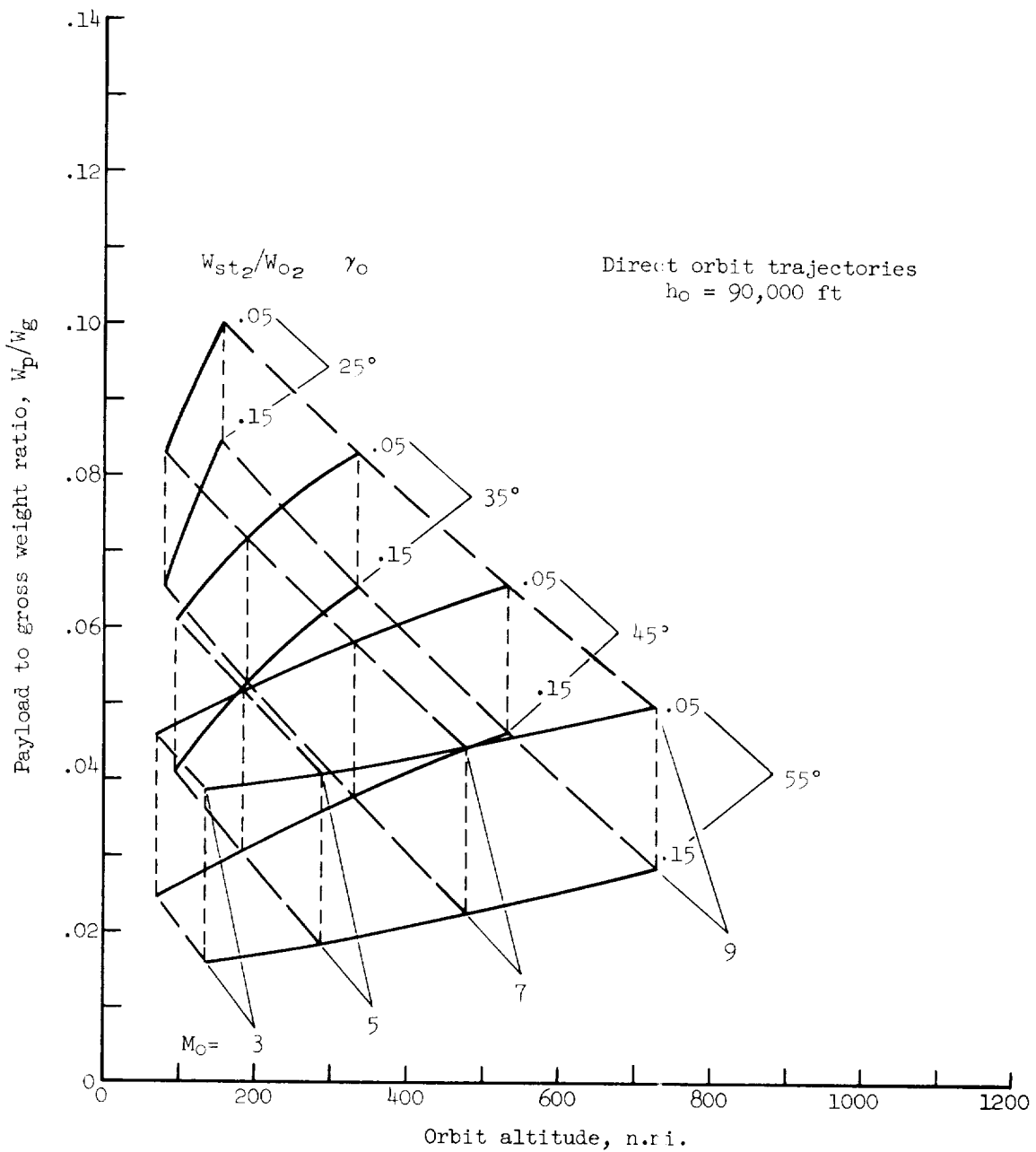
(b) First stage inert weight ratio,  $W_{st_1}/W_{o_1} = 0.15$ 

Figure 9.- Concluded.

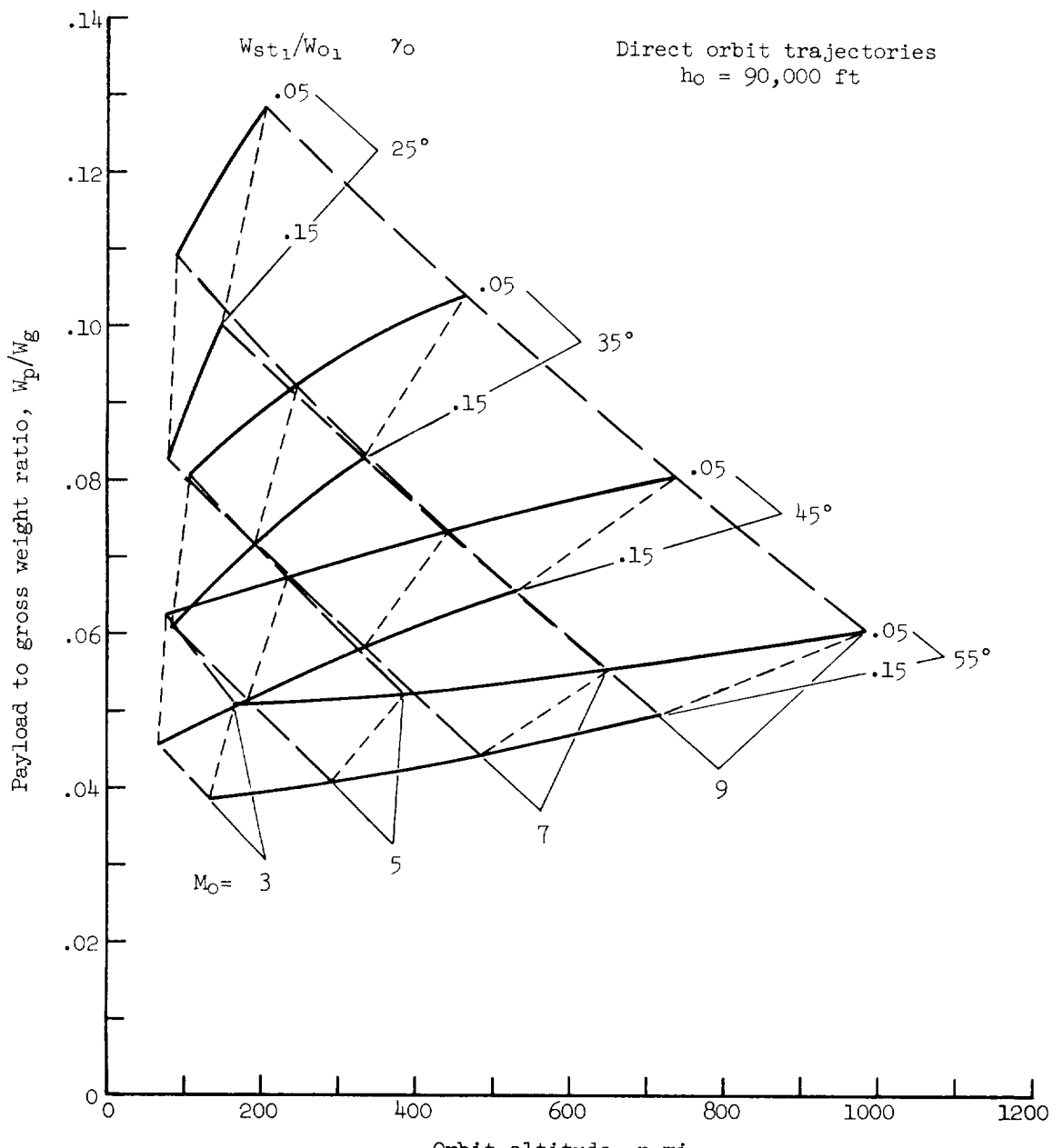
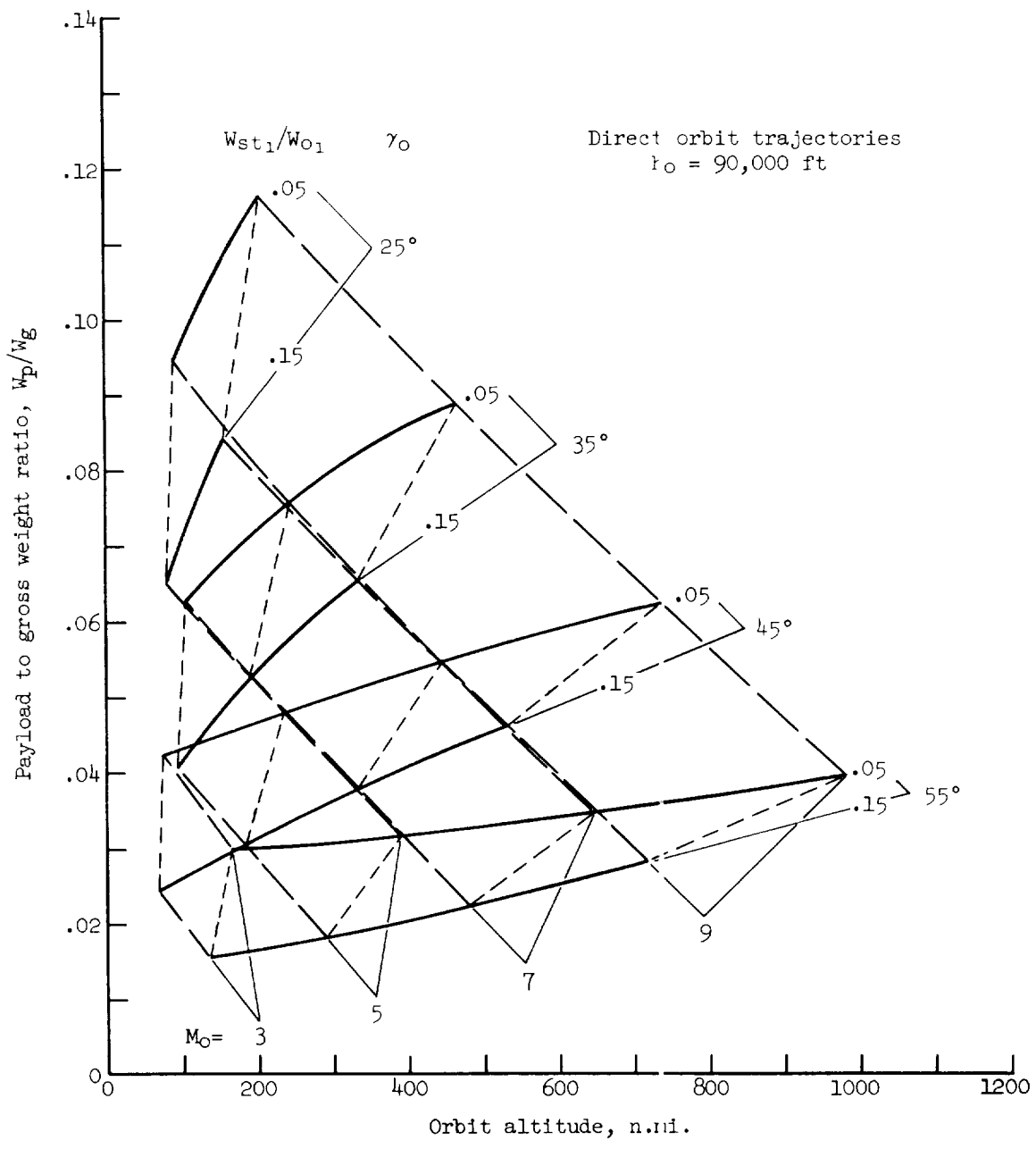
(a) Second stage inert weight ratio,  $W_{st2}/W_{02} = 0.05$ 

Figure 10.- Effect of initial angle, Mach number, orbit altitude and first stage inert weight ratio on payload ratio for  $T/W = 1.50$ .



(b) Second stage inert weight ratio,  $W_{st_2}/W_{o_2} = 0.15$

Figure 10.- Concluded.

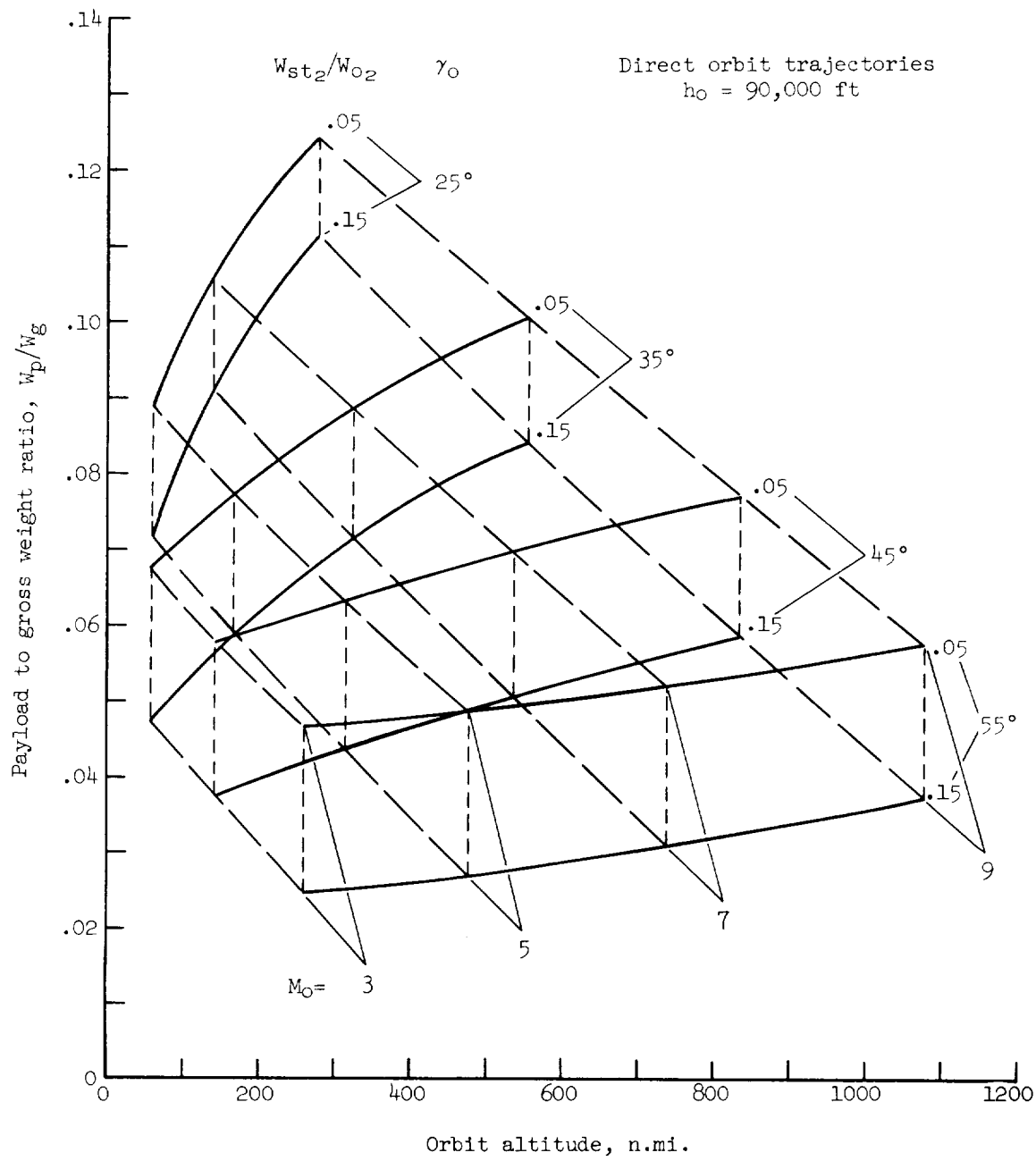
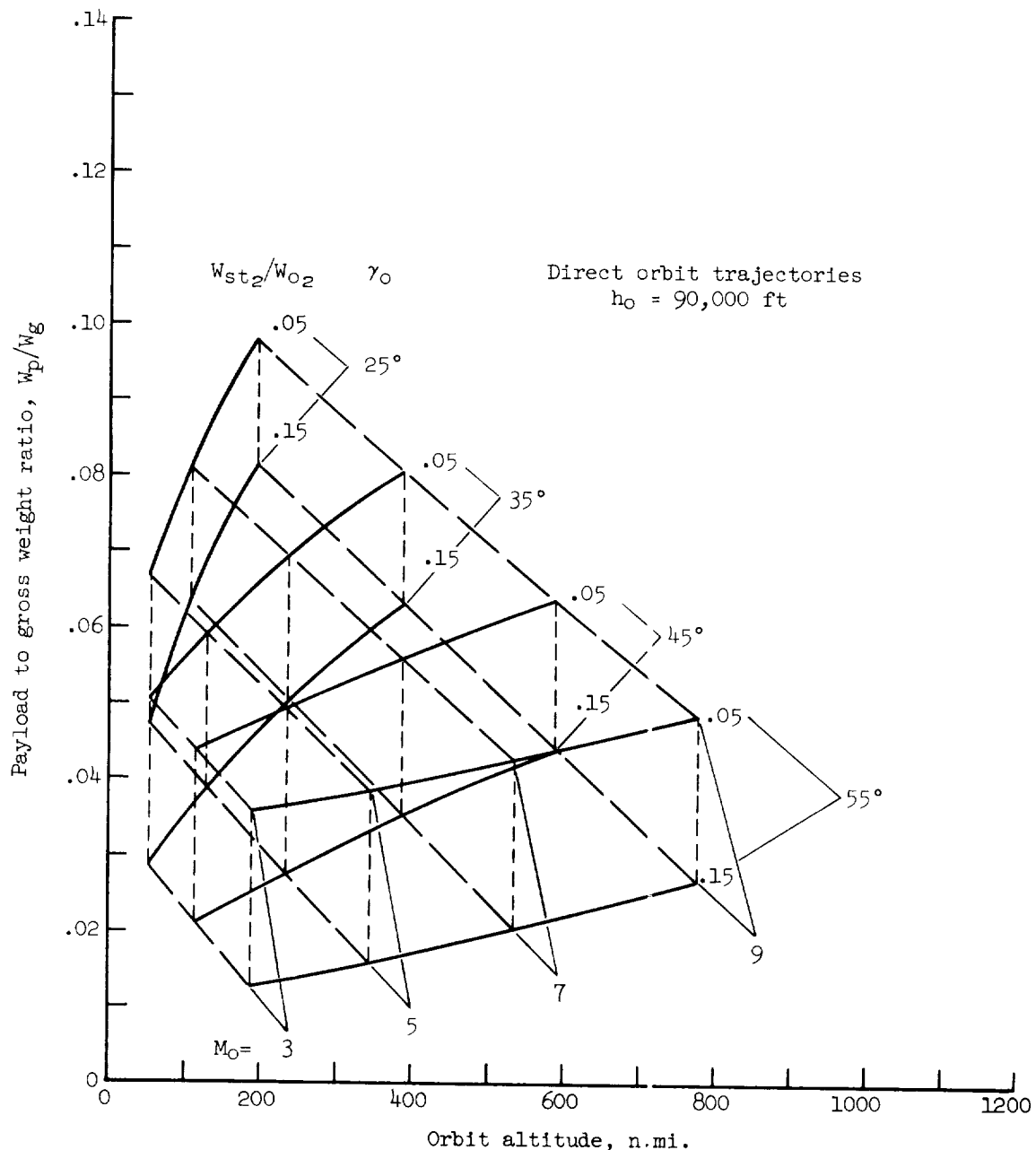


Figure 11.- Effect of initial angle, Mach number, orbit altitude and second stage inert weight ratio on payload ratio for  $T/W = 2.00$ .



(b) First stage inert weight ratio,  $W_{St,1}/W_{O,1} = 0.15$

Figure 11.- Concluded.

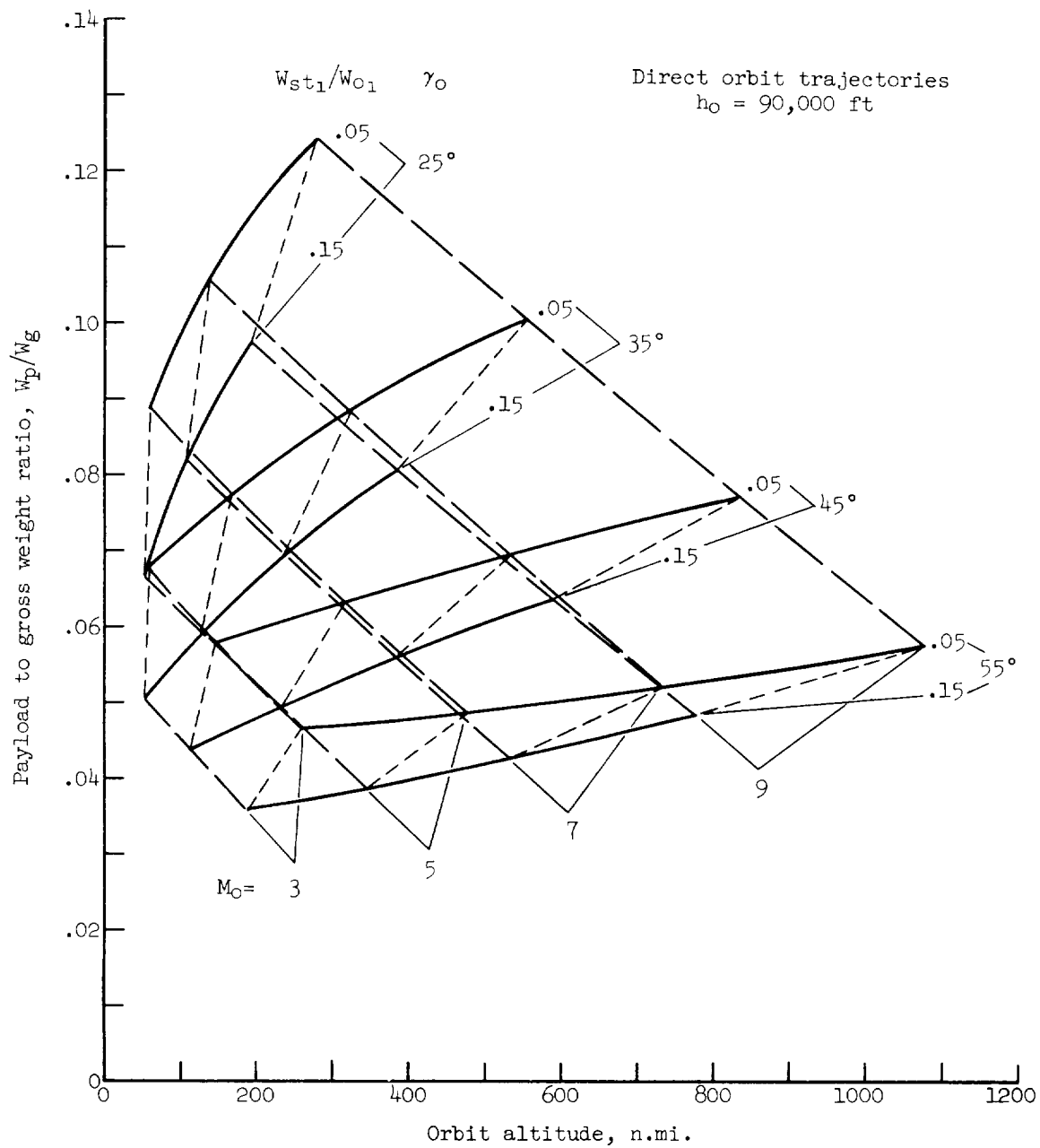


Figure 12.- Effect of initial angle, Mach number, orbit altitude and first stage inert weight ratio on payload ratio for  $T/W = 2.00$ .

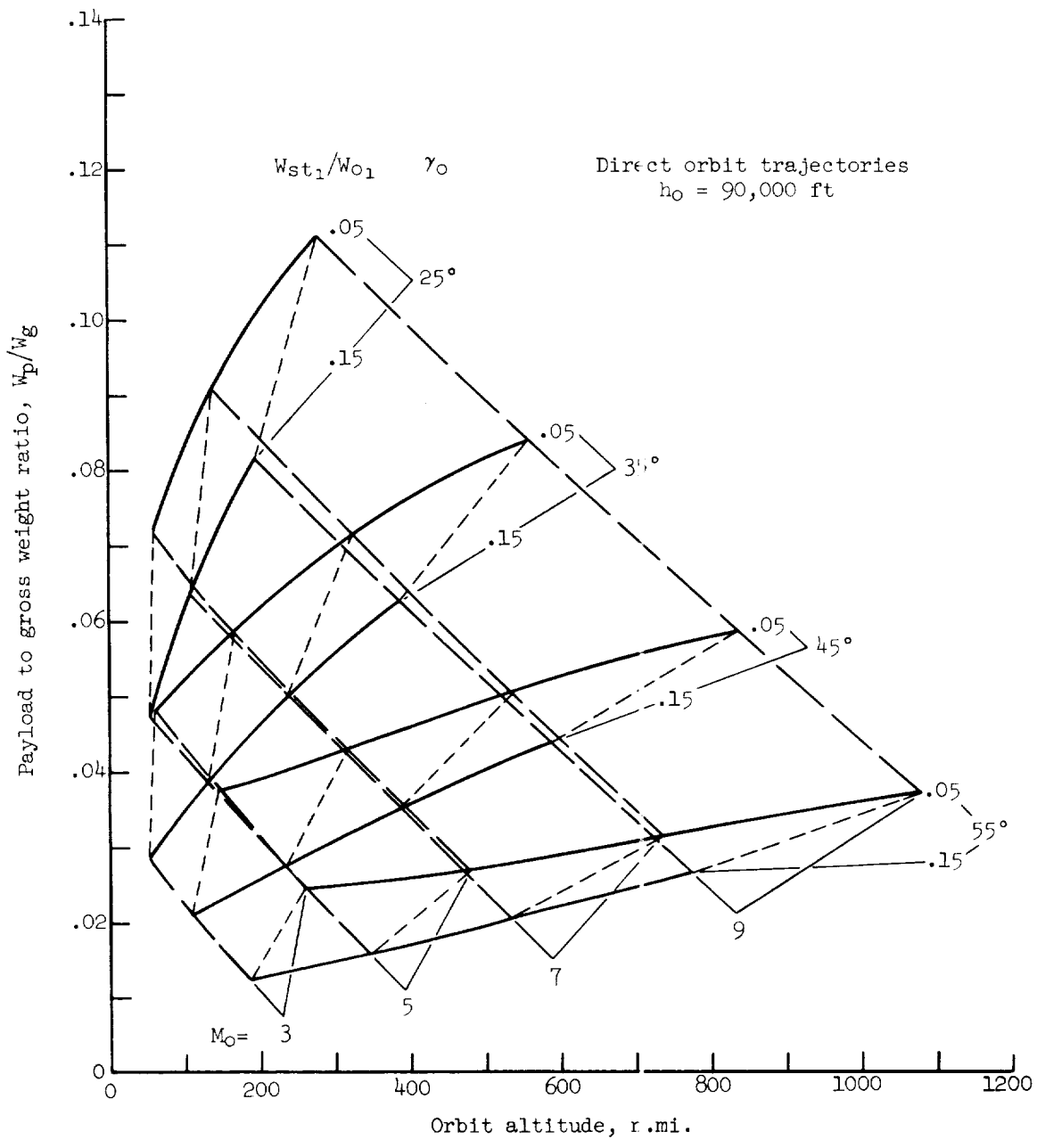
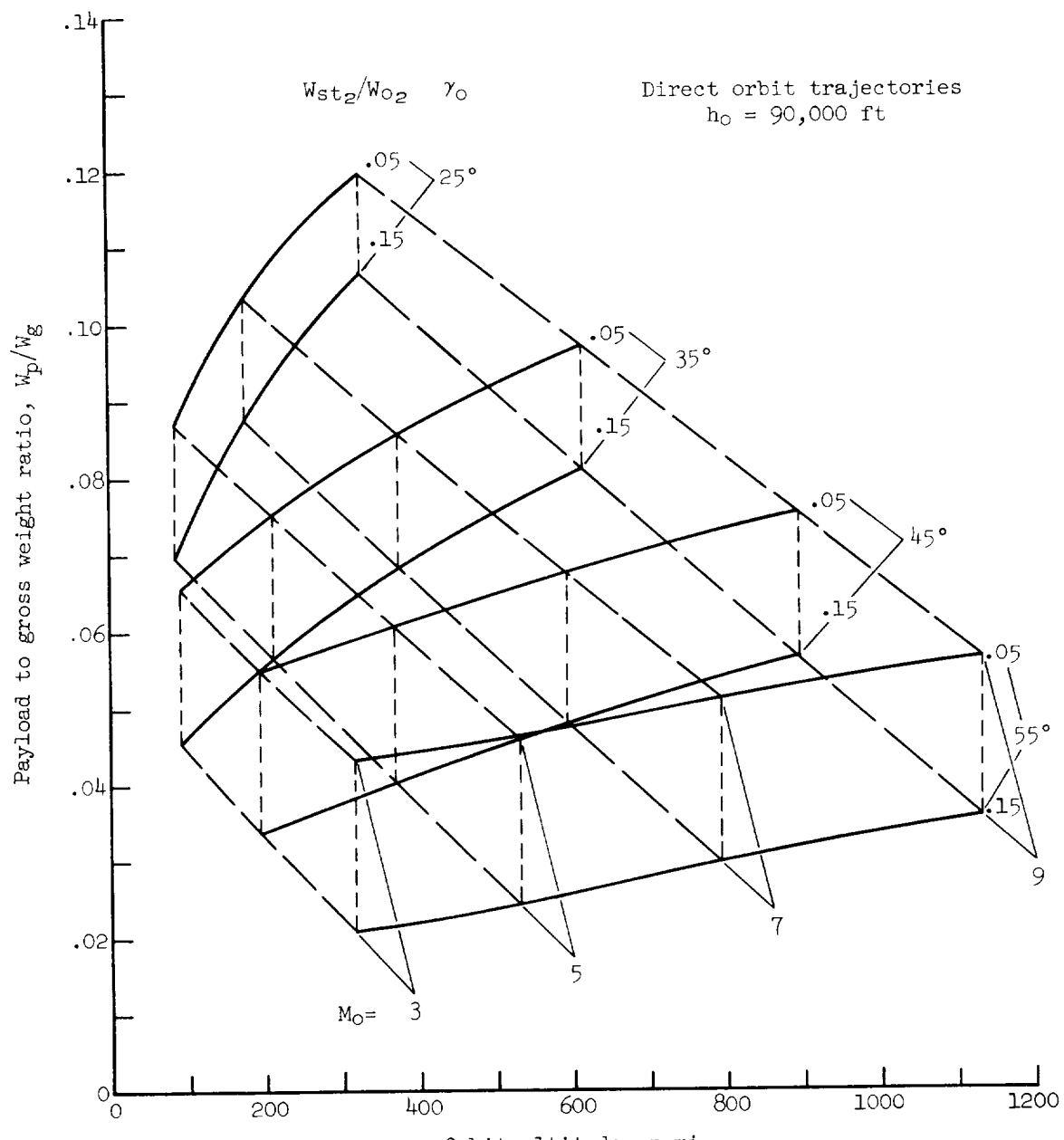


Figure 12.- Concluded.



(a) First stage inert weight ratio, W<sub>st1</sub>/W<sub>o1</sub> = 0.05

Figure 13.- Effect of initial angle, Mach number, orbit altitude and second stage inert weight ratio on payload ratio for T/W = 2.50.

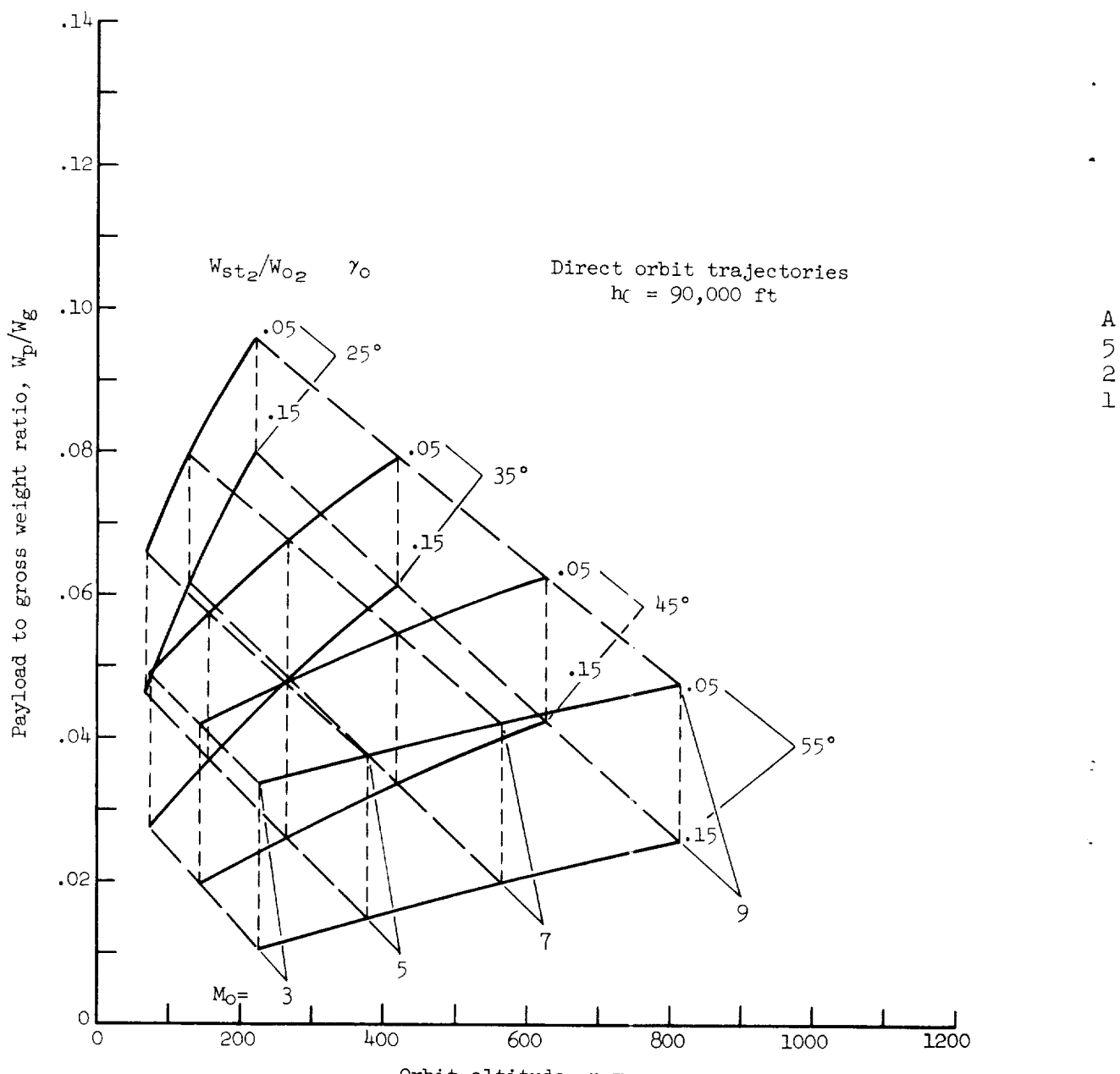
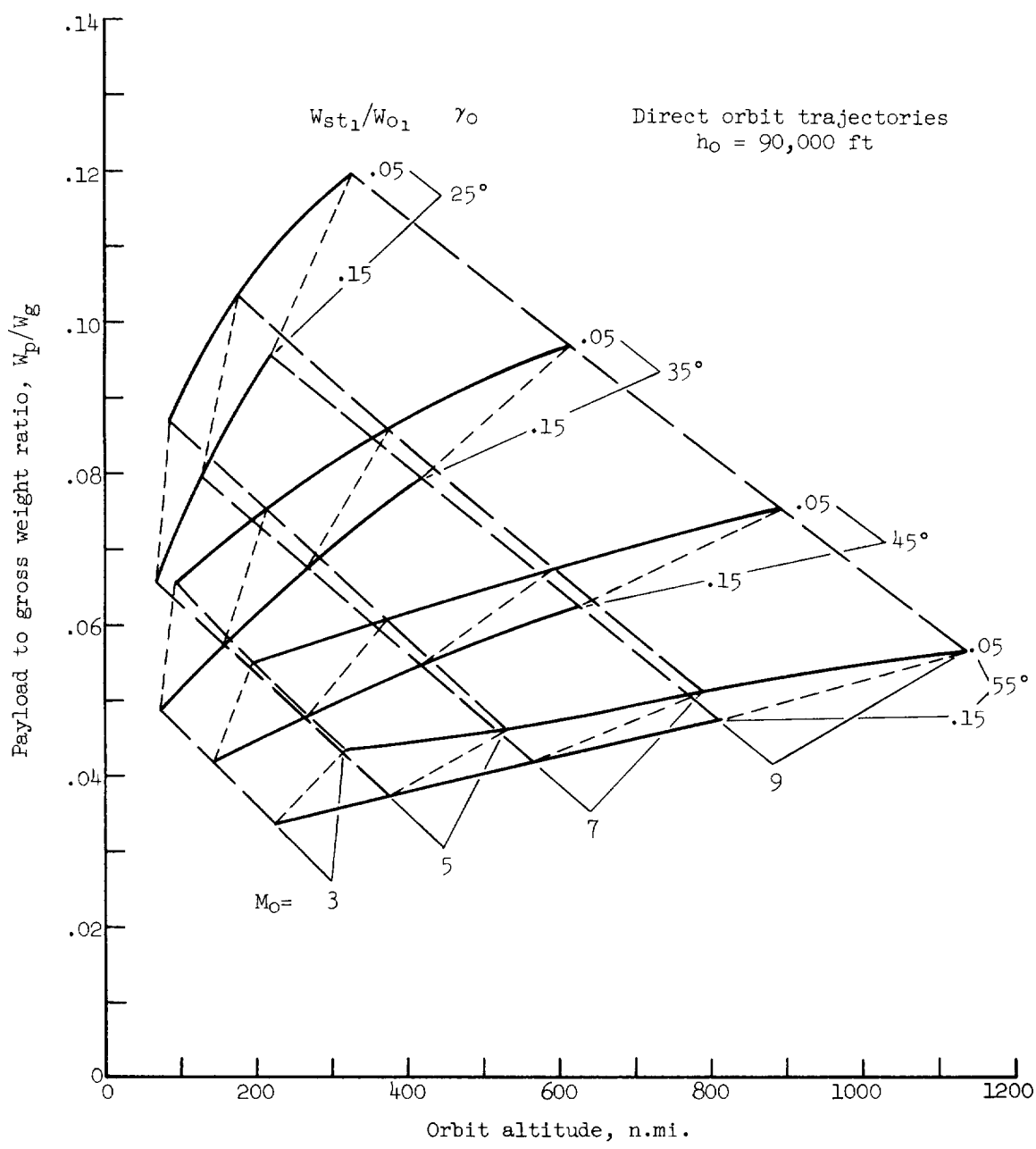
(b) First stage inert weight ratio  $W_{st_1}/W_{o_1} = 0.15$ 

Figure 13.- Concluded.



(a) Second stage inert weight ratio,  $W_{st2}/W_{o2} = 0.05$

Figure 14.- Effect of initial angle, Mach number, orbit altitude and first stage inert weight ratio on payload ratio for  $T/W = 2.50$ .

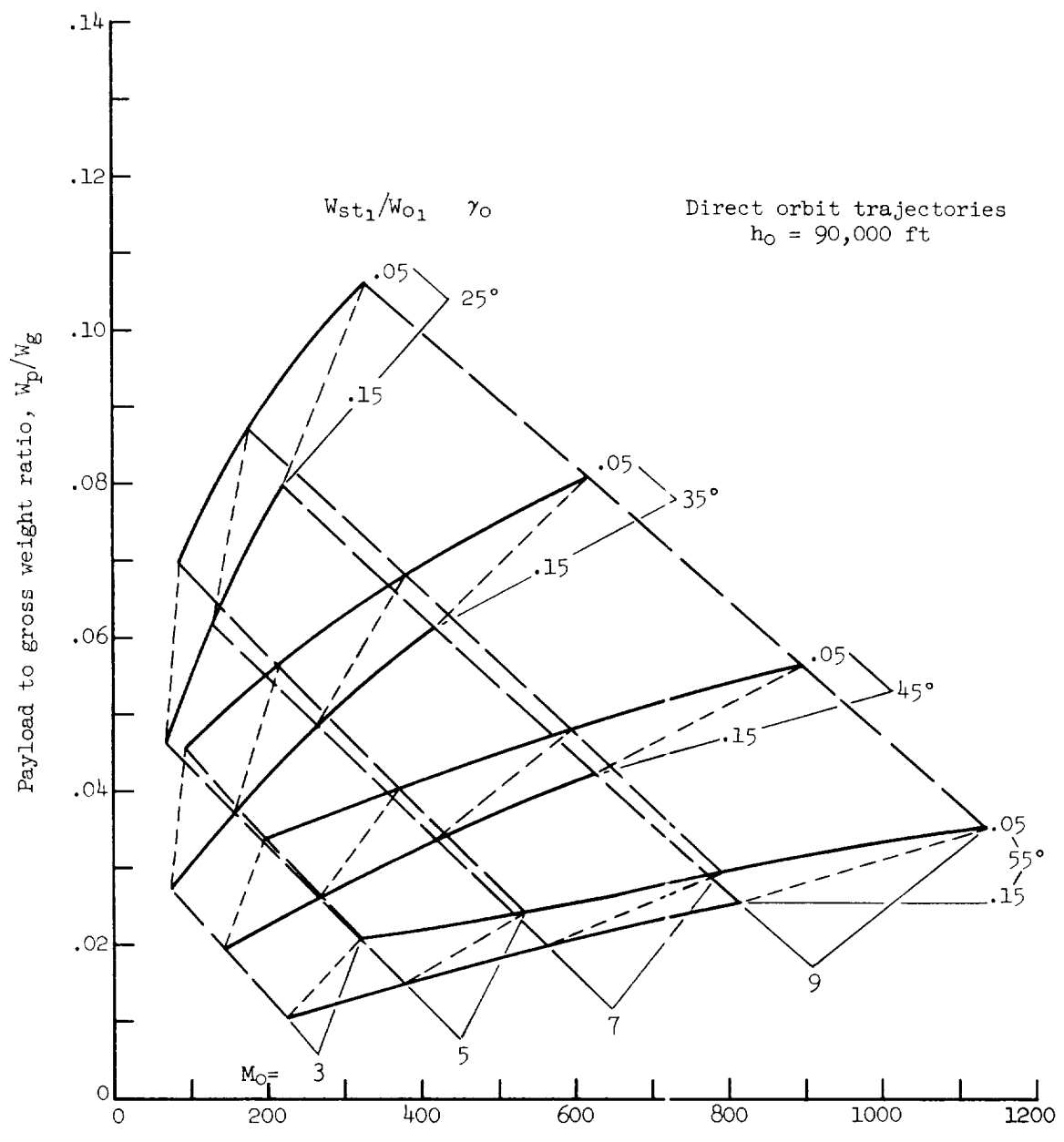


Figure 14.- Concluded.

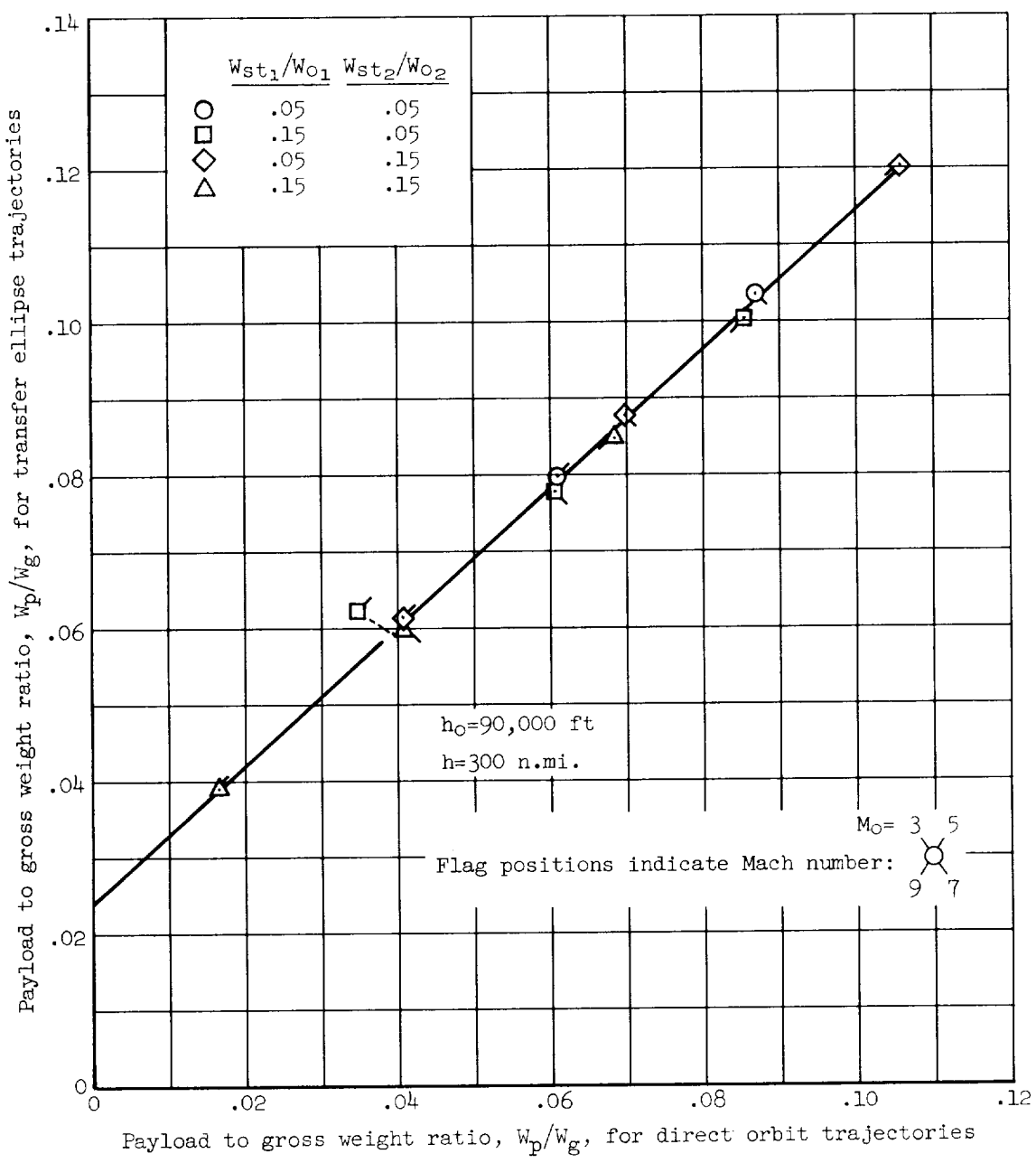
(a) Thrust-weight ratio,  $T/W = 1.50$ 

Figure 15.- Payload ratio variation with trajectory method.

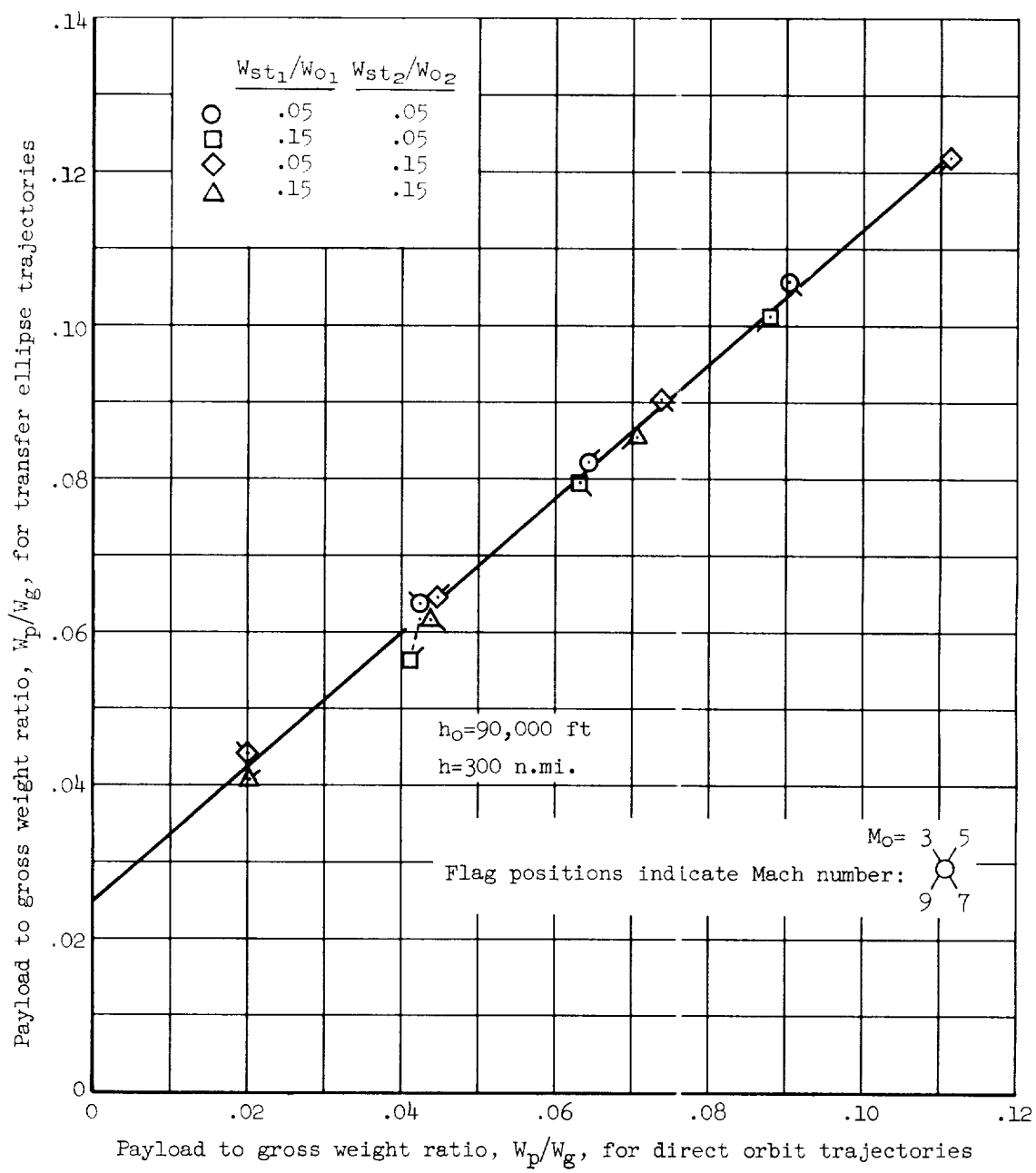
(b) Thrust-weight ratio,  $T/I = 2.00$ 

Figure 15.- Continued.

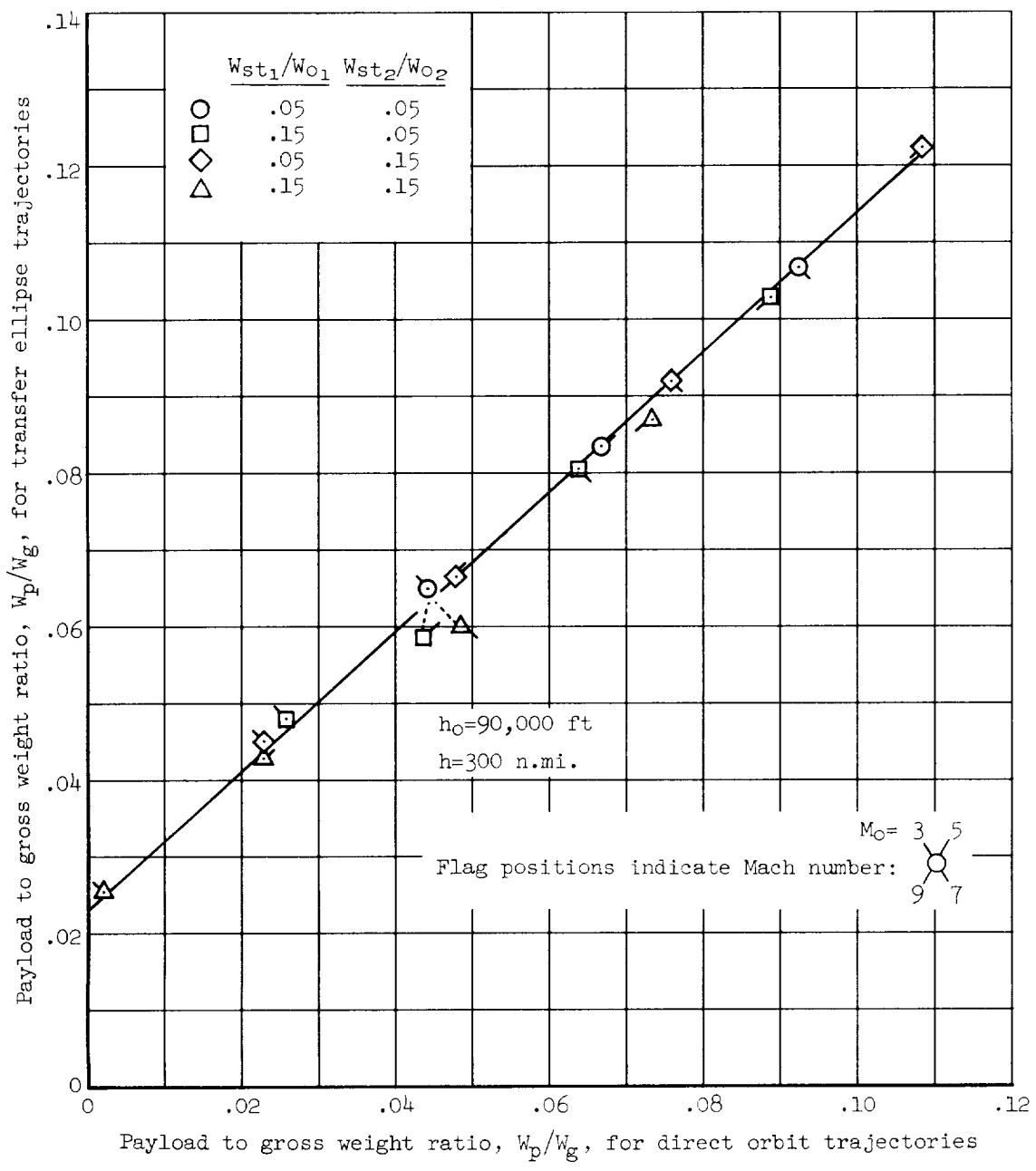
(c) Thrust-weight ratio,  $T/W = 2.50$ 

Figure 15.- Concluded.

